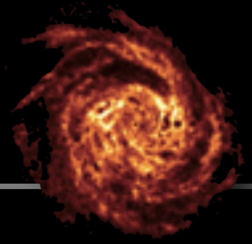

Spectral Line Interferometry

science & principles

Marc Verheijen

university of groningen / Kapteyn Astronomical Institute

Detailed Anatomy of GALaxies

ERIS 2013, 9-13 Sept 2013 - Dwingeloo

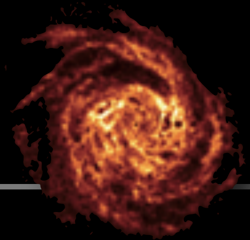

overview

- Focus on science with spectral lines in *radio* domain
  - for the mm-domain, see lecture by Bremer
- The 21cm line of atomic hydrogen
  - emission / absorption
  - selected science topics
- Astrophysical (Mega)MASERs
  - OH, H_2O, SiO, methanol
  - selected science examples
- Radio Recombination Lines
  - science and a few examples

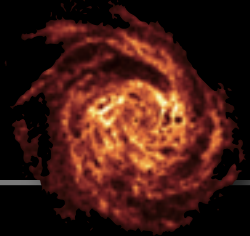

the HI 21-cm line of Hydrogen

Predicted to be observable by Van de Hulst (1944)
First detected by Ewen & Percell (1951)

magnetic dipole transition

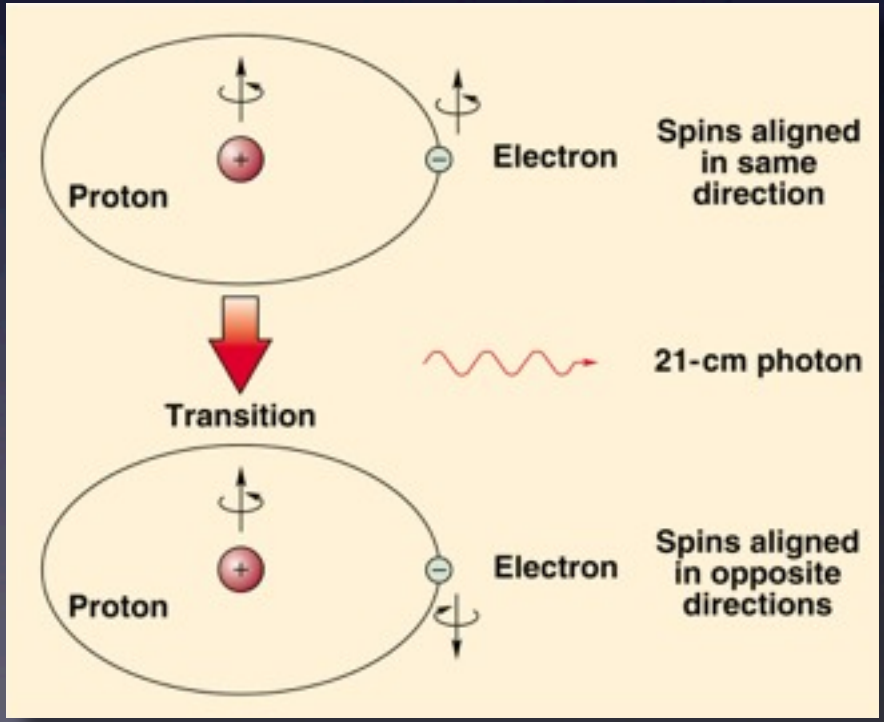

$$\nu_{1\to0} = \frac{8}{3}\; g_p \; (m_e/m_p)\; \alpha^2 \; R_M c$$

$$= 1420.40575177 \quad [\text{ MHz }]$$

where g_p = *g-factor of proton*
α = *fine-structure constant*
$R_M c$ = *Rydberg constant*

the HI 21-cm line of Hydrogen

- Coefficient of emission : $$A_{10} = \frac{64\pi^4}{3hc^3} \nu_{10}^3 \; |\mu^*_{10}|^2$$
$$= 2.85 \times 10^{-15} \quad [s^{-1}]$$
where $|\mu^*_{10}|$ = *Bohr magneton*

- Thus, the radiative half-life $t_{½} = 1/A_{10} = 3.51 \times 10^{14}$ [s]
$\approx$ 11 million years

This implies that even the low-density ISM can excite this transition by means of collisions.

the HI 21-cm line of Hydrogen

- Spin temperature T_{spin} is defined as

$$\frac{\eta_1}{\eta_0} \equiv \frac{g_1}{g_0} \exp\left(-\frac{h\nu_{10}}{kT_{spin}}\right) = 3 \exp\left(-\frac{0.0682}{T_{spin}}\right)$$

where g_1 and g_0 are the statistical weights of the two levels (3:1 for HI)

For T_{spin} = 100 [K], $\eta_1 = 3\eta_0$ and $\eta_{HI} = 4\eta_0$

- The line opacity coefficient is given by:

$$\kappa_\nu = \frac{h\nu_{10}}{c} \eta_0 B_{01} \left[1 - \exp\left(-\frac{h\nu_{10}}{kT_{spin}}\right)\right]$$

$$= \frac{c^2}{8\pi\nu_{10}^2} \frac{g_1}{g_0} \frac{\eta_{HI}}{4} A_{10} \left[1 - \exp\left(-\frac{h\nu_{10}}{kT_{spin}}\right)\right]$$

the HI 21-cm line of Hydrogen

or $$\kappa_\nu \approx \frac{3hc\lambda A_{10}}{32\pi k} \frac{\eta_{HI}}{T_{spin}}$$

The optical depth τ_ν follows from integration along the line-of-sight and multiplying with the line shape $\varphi(\nu)$

given $$\int_{los} \eta_{HI}(s)\, ds = N_{HI} \quad \text{and} \quad \int_{line} \varphi(\nu) d\nu = 1$$

it follows
$$\tau_\nu = \frac{3hc\lambda A_{10}}{32\pi k} \frac{N_{HI}}{T_{spin}} \varphi(\nu)$$

For a Gaussian line, the optical depth at line center is

$$\tau_0 = \frac{N_{HI}\,[\mathrm{cm}^{-2}]}{4.19\times10^{17}\; T_{spin}^{3/2}\,[\mathrm{K}]}$$

the HI 21-cm line of Hydrogen

For $N_{HI} = 2 \times 10^{20}$ [cm^{-2}] :

CNM : $T_{spin} \approx$ 100 K → $\tau_0 \approx 1$ optically thick
WNM : $T_{spin} \approx$ 10.000 K → $\tau_0 \ll 1$ optically thin

- Writing τ_ν and $\varphi(\nu)$ in terms of velocity, and integrating over the line profile yields:

$$\int_{line} \tau_\nu \, dV = \frac{N_{HI} \; / \; T_{spin}}{1.83 \times 10^{18} \; [\mathrm{cm}^{-2} \, \mathrm{K}^{-1}]} \quad [\mathrm{km/s}]$$

or

$$N_{HI} \; [\mathrm{cm}^{-2}] = 1.83 \times 10^{18} \int_{line} T_{spin}[\mathrm{K}] \; \tau_\nu \; dV[\mathrm{km/s}]$$

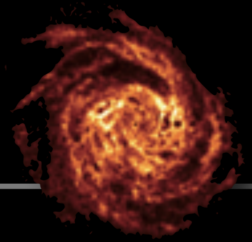

the HI 21-cm line of Hydrogen

The observed brightness temperature of an HI cloud can be defined and written as:

$$T_b = (T_{spin} - T_{BG})(1 - e^{-\tau(\nu)})$$

with T_{BG} = temperature of background source

If $(T_{spin} - T_{BG}) > 0 \rightarrow$ emission line

$(T_{spin} - T_{BG}) < 0 \rightarrow$ absorption line

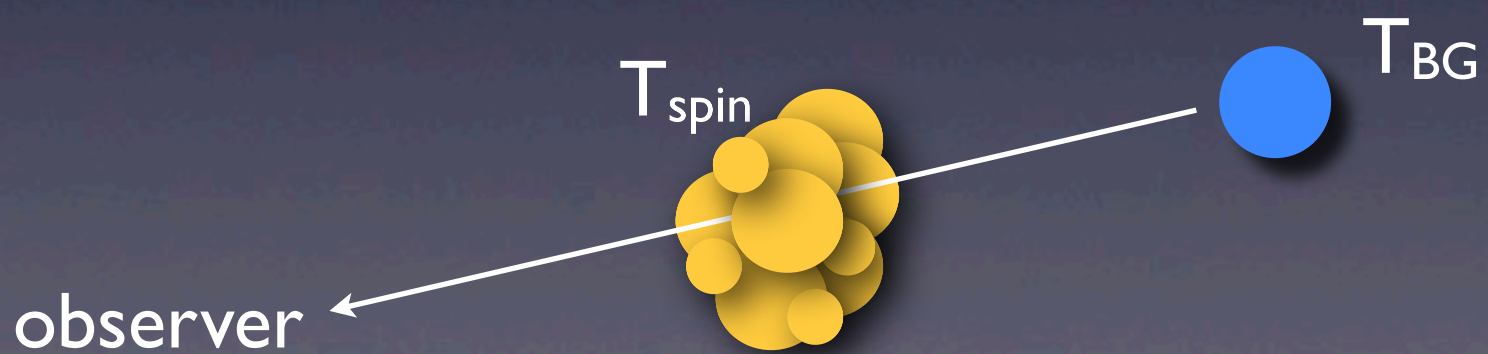

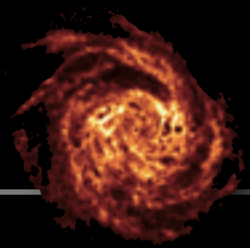

the HI 21-cm line of Hydrogen

- If $T_{spin} \gg T_{BG}$ (e.g. $T_{BG} = 2.73$ K) :

$$T_b = (T_{spin} - T_{BG})(1 - e^{-\tau(\nu)}) \approx T_{spin}\,(1 - e^{-\tau(\nu)})$$

or $T_{spin} = T_b \,/\, (1 - e^{-\tau(\nu)})$

$$\rightarrow \; N_{HI}\,[\mathrm{cm}^{-2}] = 1.83\mathrm{x}10^{18} \int_{line} \frac{T_b\,[\mathrm{K}]\,\tau_\nu}{1 - e^{-\tau(\nu)}}\, dV[\mathrm{km/s}]$$

In the optically thin regime ($\tau_\nu \ll 1$) :

$$N_{HI}\,[\mathrm{cm}^{-2}] = 1.83\mathrm{x}10^{18} \int_{line} T_b\,[\mathrm{K}]\; dV\,[\mathrm{km/s}]$$

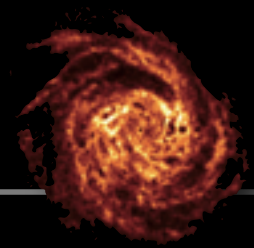

the HI 21-cm line of Hydrogen

- For a Gaussian synthesized beam, the relation between the measured flux density and temperature is:

$$1\ [\mathrm{K}] = \frac{605.7}{\theta_x\,\theta_y}\left(\frac{\nu_0}{\nu}\right)^2 = 605.7\,\frac{(1+z)^2}{\theta_x\,\theta_y}\ [\mathrm{mJy}]$$

where θ_x, θ_y = FWHM in arcsec of a Gaussian beam
ν_0, ν = rest and observed frequency of HI line

Note that the column density sensitivity can be improved by smoothing the data to a larger beam.

the HI 21-cm line of Hydrogen

- If $T_{BG} < T_{spin} < T_{src}$: HI line is seen in absorption against bright source

$$T_b = (T_{spin} - T_{src})(1 - e^{-\tau(\nu)}) < 0$$

$$T_{spin} = \frac{T_b}{1 - e^{-\tau(\nu)}} + T_{src}$$

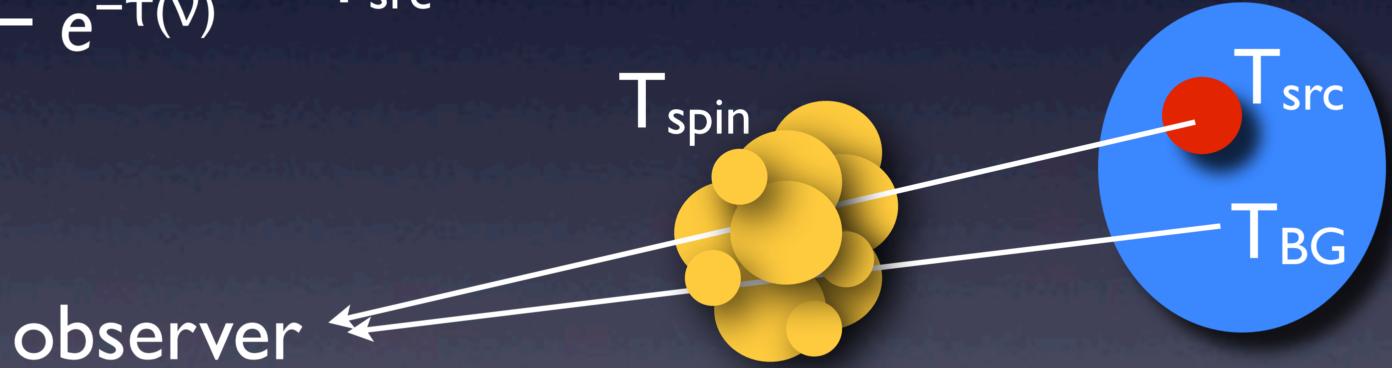

Measuring the temperatures both on/off source and on/off line, allows determination of both τ_ν and T_{spin} and thus N_{HI} .

the HI 21-cm line of Hydrogen

Taking cosmological effects into account:

$$N_{HI}\,[\mathrm{cm}^{-2}] = 1.83\mathrm{x}10^{18}\ (1+z)^2 \int_{line} T_b\,[\mathrm{K}]\,dV\,[\mathrm{km/s}]$$

$$M_{HI}\,[M_{sun}] = 2.36\mathrm{x}10^{5}\ \frac{D_{lum}^2\,[\mathrm{Mpc}]}{1+z} \int_{line} S_v\,[\mathrm{Jy}]\,dV\,[\mathrm{km/s}]$$

More details on the radiative process of the HI line can be found in many places online. E.g.:

http://www.cv.nrao.edu/course/astr534/HILine.html

http://astro.berkeley.edu/~ay216/08/NOTES/Lecture10-08.pdf

HI disks reach far into the Dark Matter halos

NGC 2403

Fraternali et al (2001)

NGC 6946

Boomsma (2007)

NGC 5055

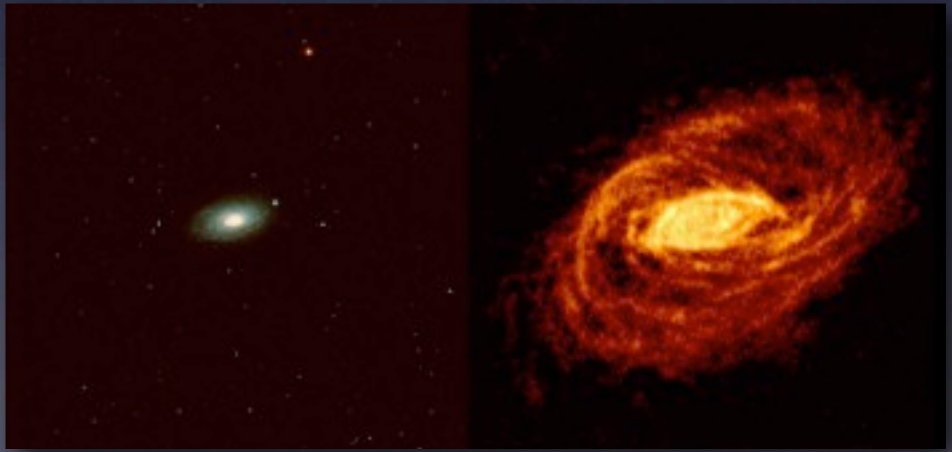

Battaglia et al (2005)

Messier 31

Braun et al

HI data from Westerbork

typical HI data products

HI column density map

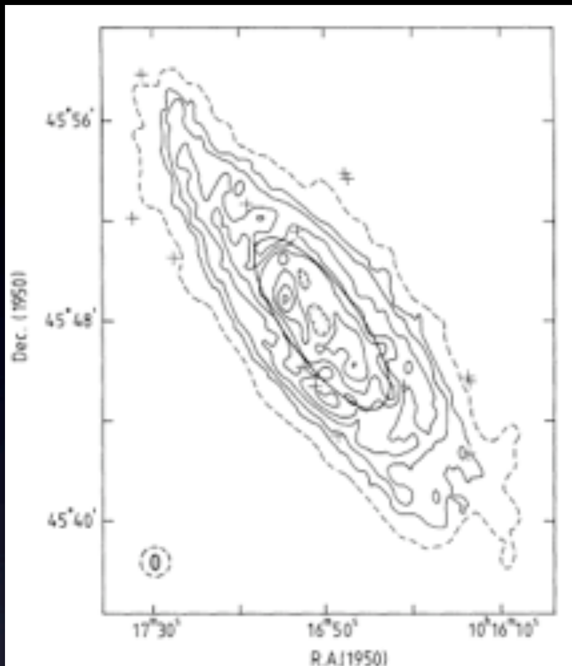

velocity field

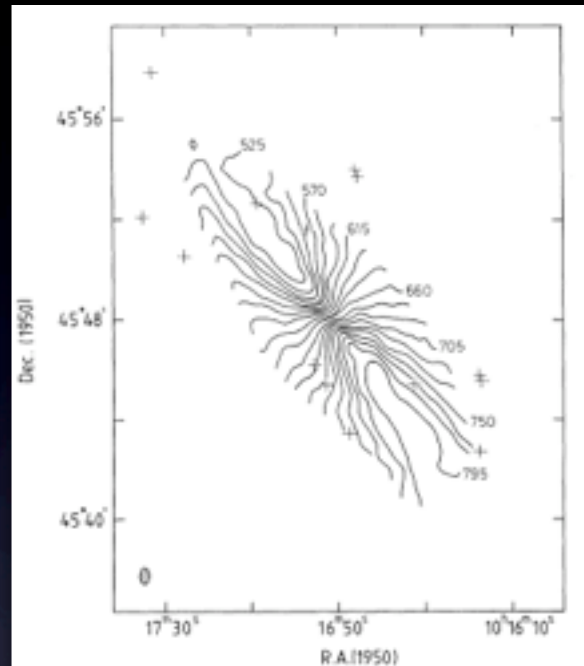

luminosity profile

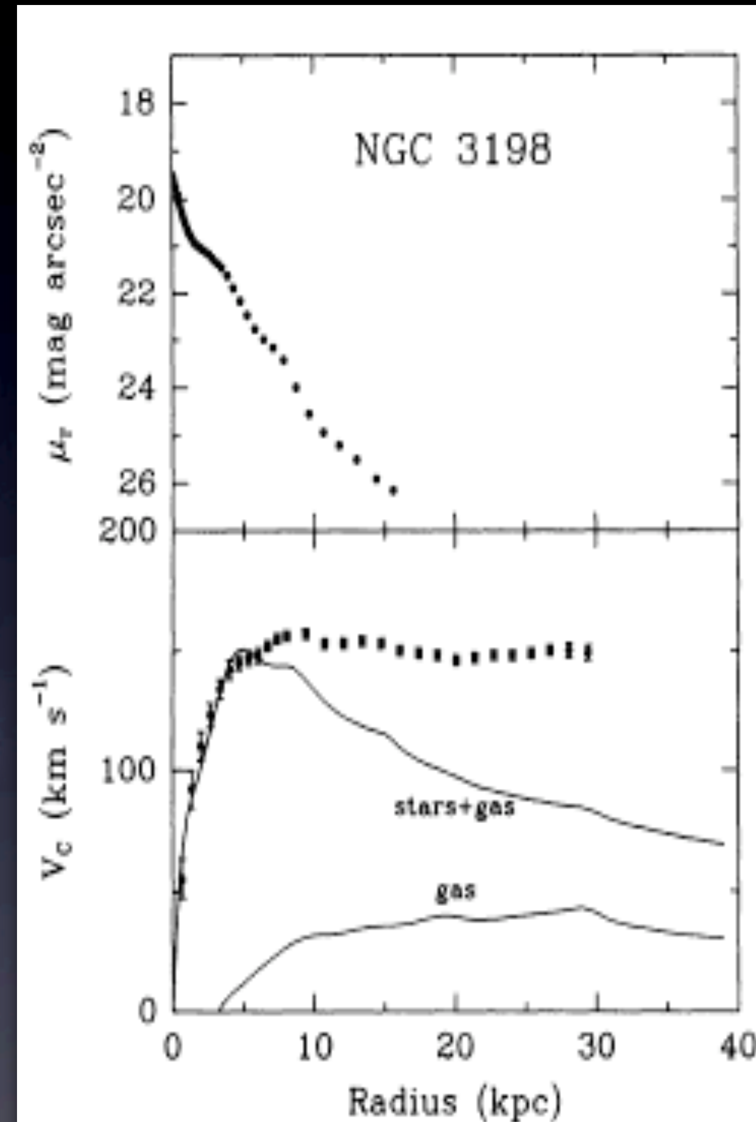

radial HI distribution

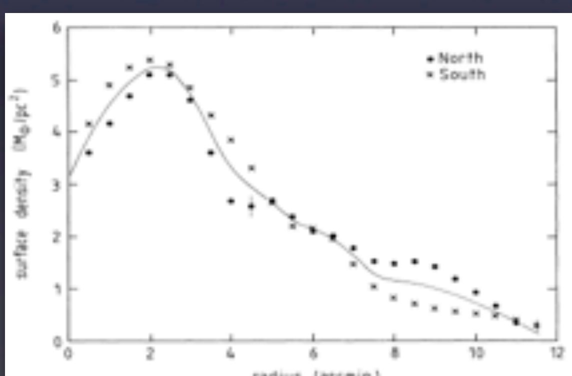

position-velocity diagram

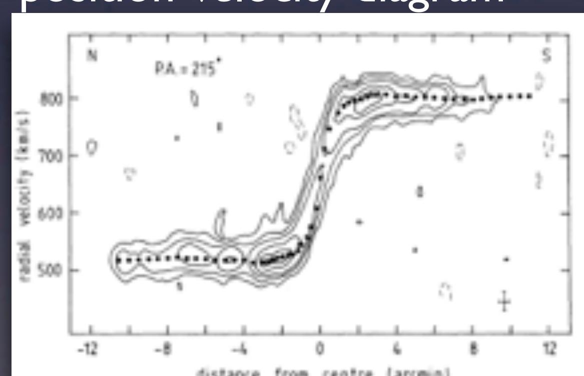

Begeman (1987)

dark matter ‘conspires’ with baryons to keep outer rotation curve flat

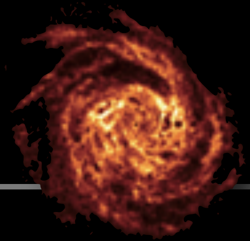

major HI imaging surveys

Targeted Surveys of selected samples:

• WHISP (350)	northern spirals with F>100 mJy
• VIVA (53)	SFR-selected Virgo spirals
• UMa (85)	Ursa Major group with M_B< -18.5
• THINGS (34)	HI follow-up of SINGS sample
• LittleTHINGS (42)	Local dIm and BCDs
• FIGGS (47)	Faint Irregular galaxies
• ATLAS^{3D} (166)	HI follow-up of northern early-types
• HALOGAS (22)	the deepest HI survey of spirals
• VLA-ANGST (36)	HI follow-up of HST/ACS survey

Blind Surveys of different environments:

- Coma (WSRT)
- Perseus-Pisces (VLA)
- Ursa Major (VLA)
- CVn (WSRT)

21cm spectral-line imaging - Dwarfs

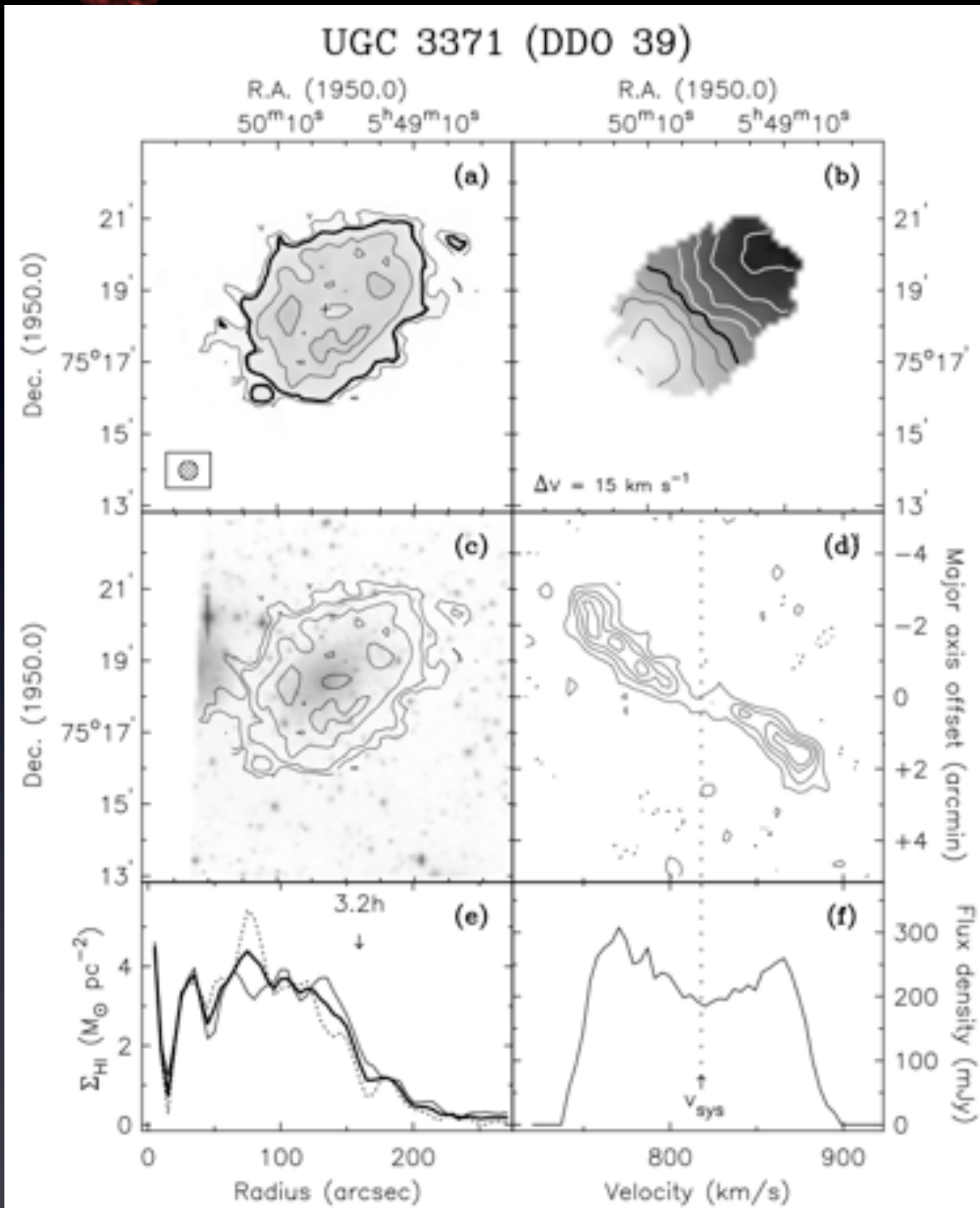

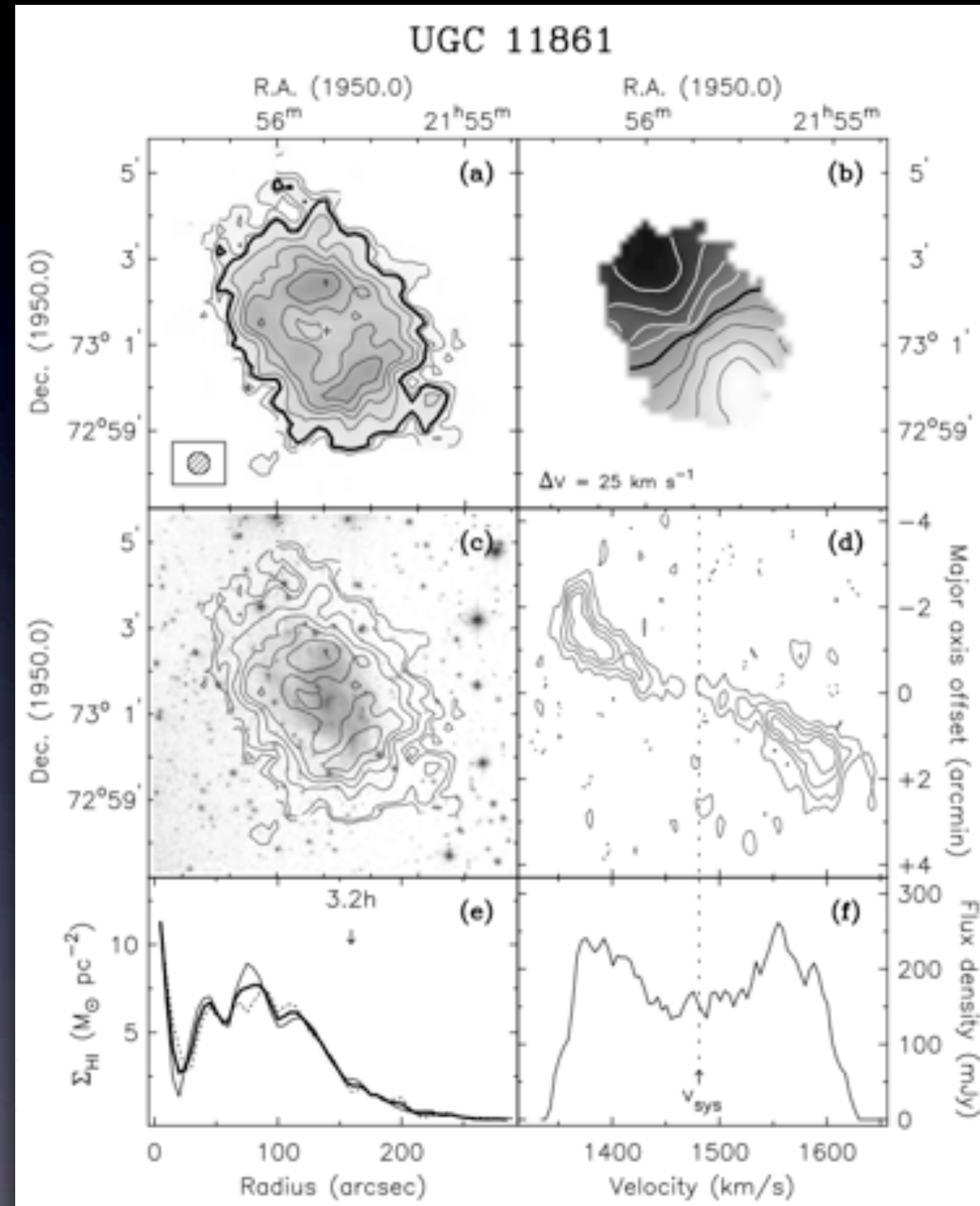

Swaters et al (2002)

21cm spectral-line imaging - Ursa Major

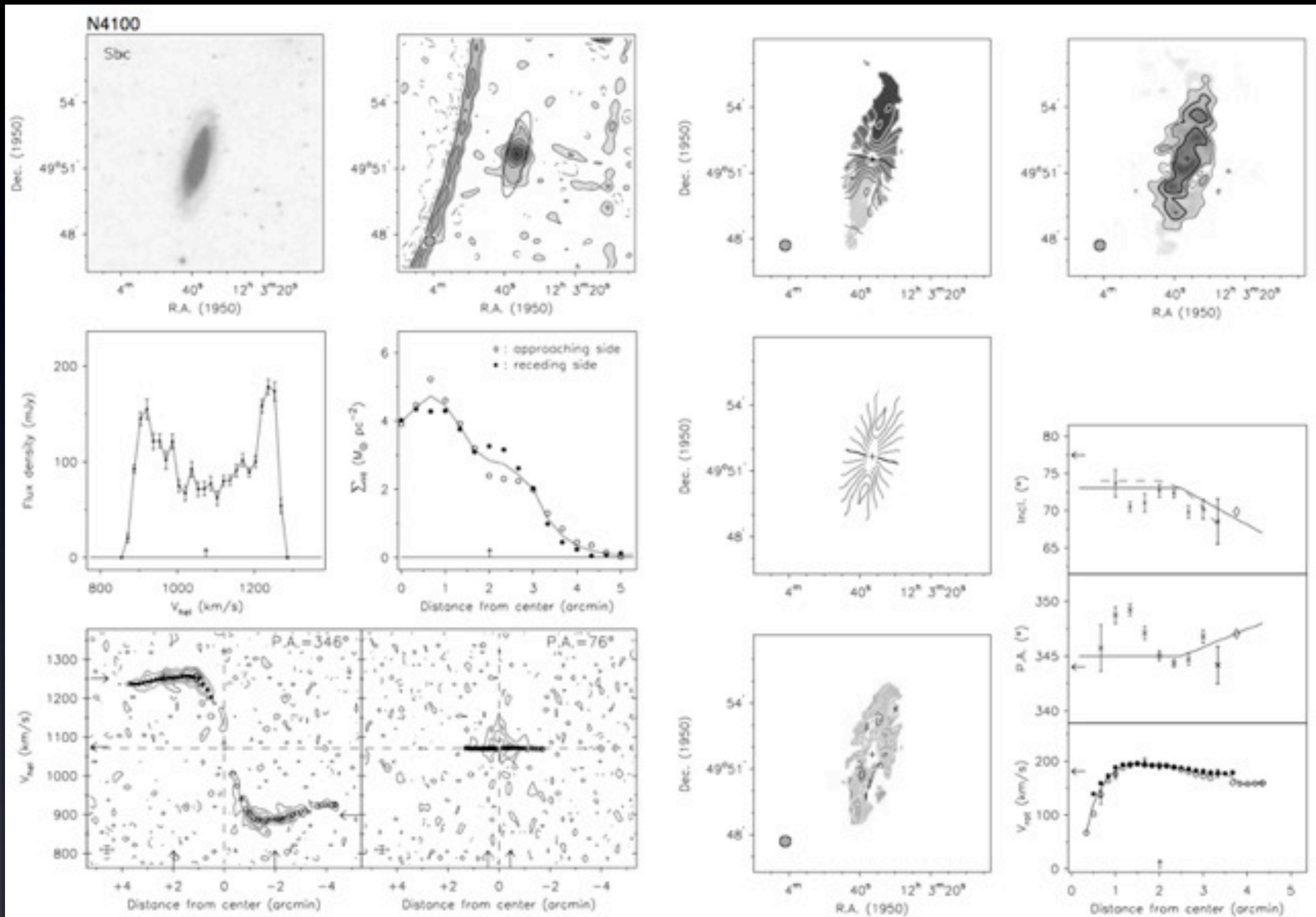

Verheijen & Sancisi (2001)

21cm spectral-line imaging - Ursa Major

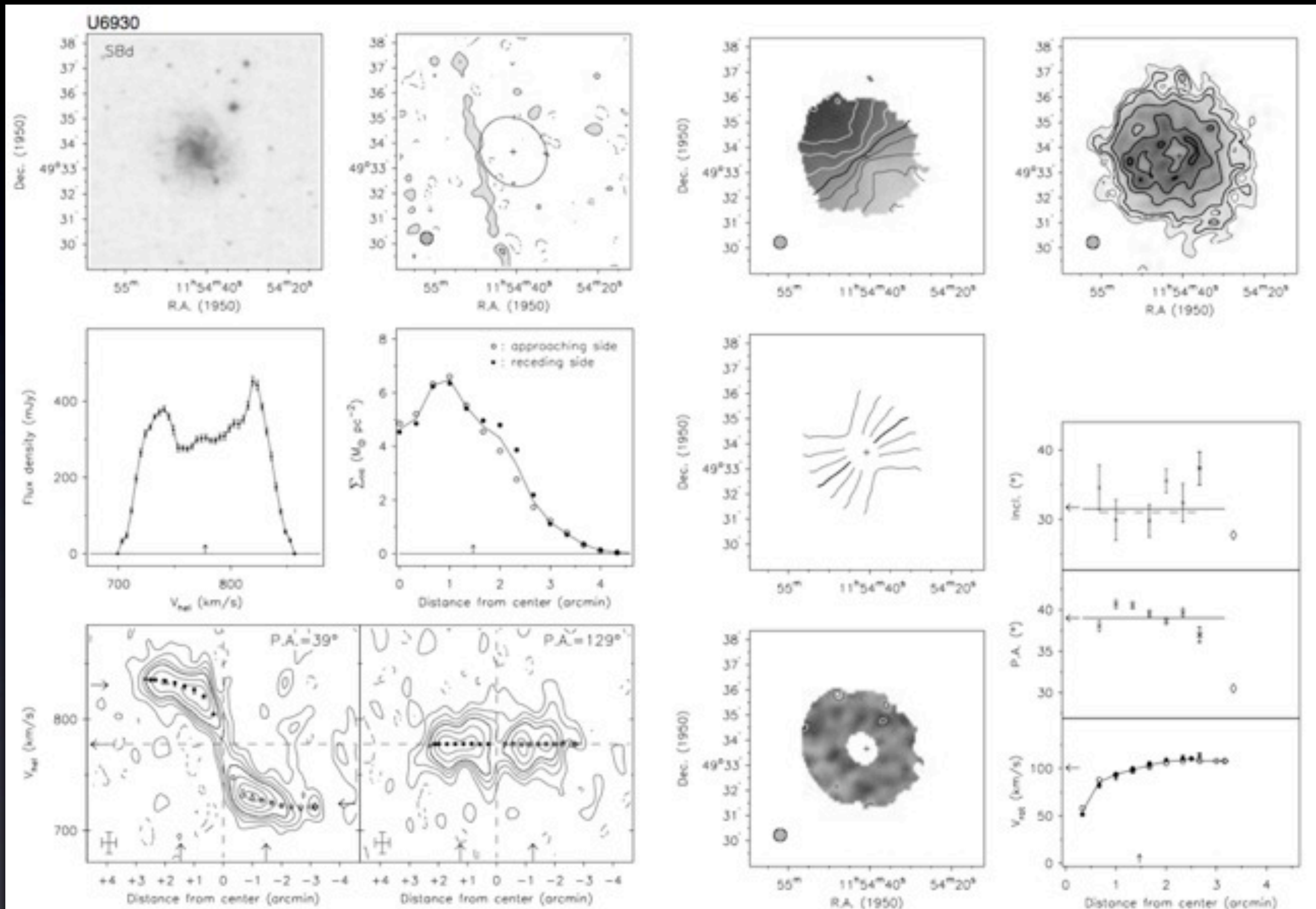

Verheijen & Sancisi (2001)

21cm spectral-line imaging - massive spirals

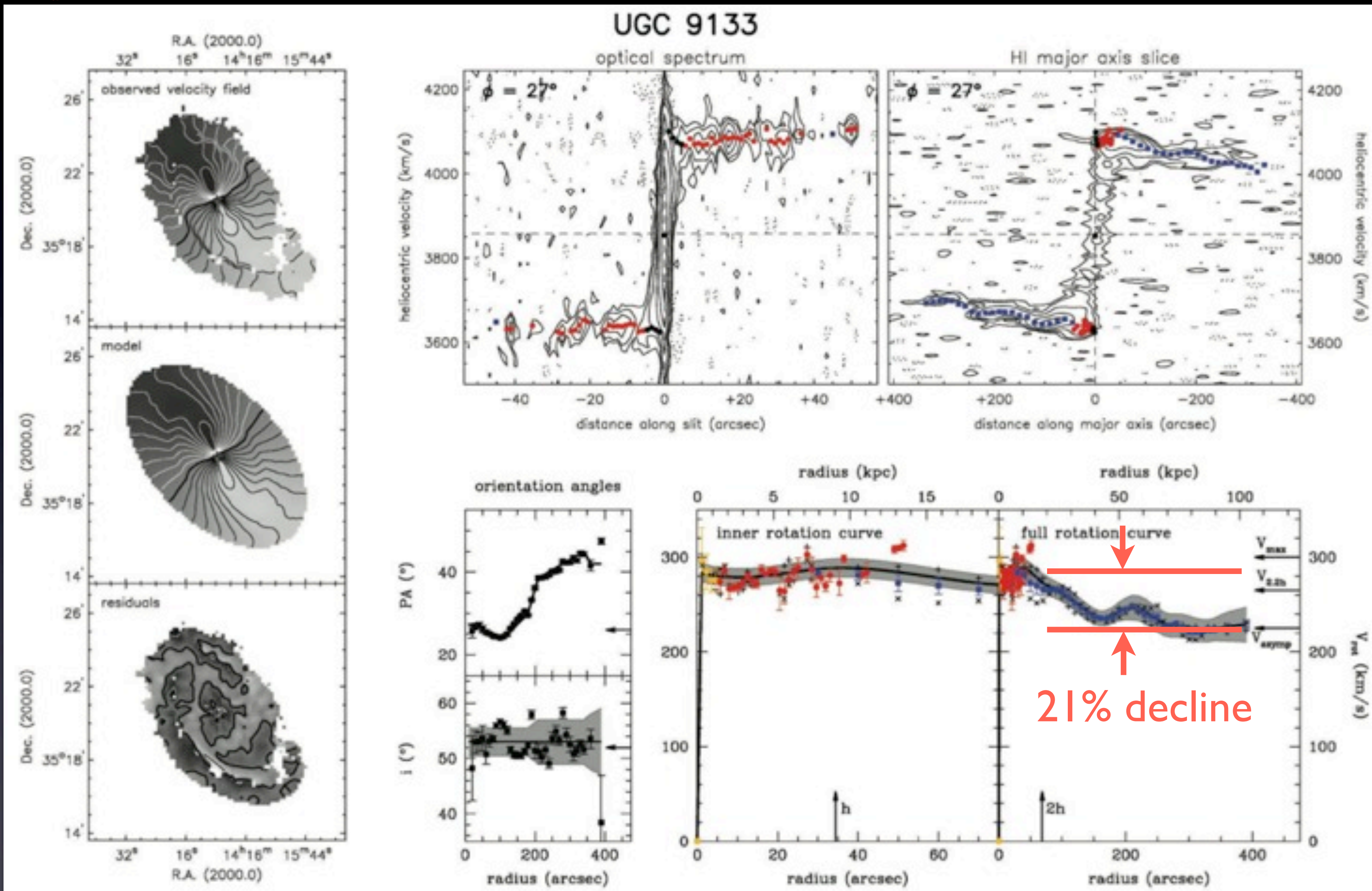

Noordermeer et al (2005)

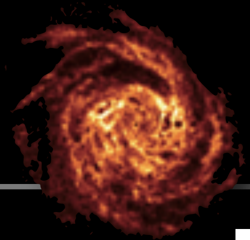

21cm spectral-line imaging - THINGS

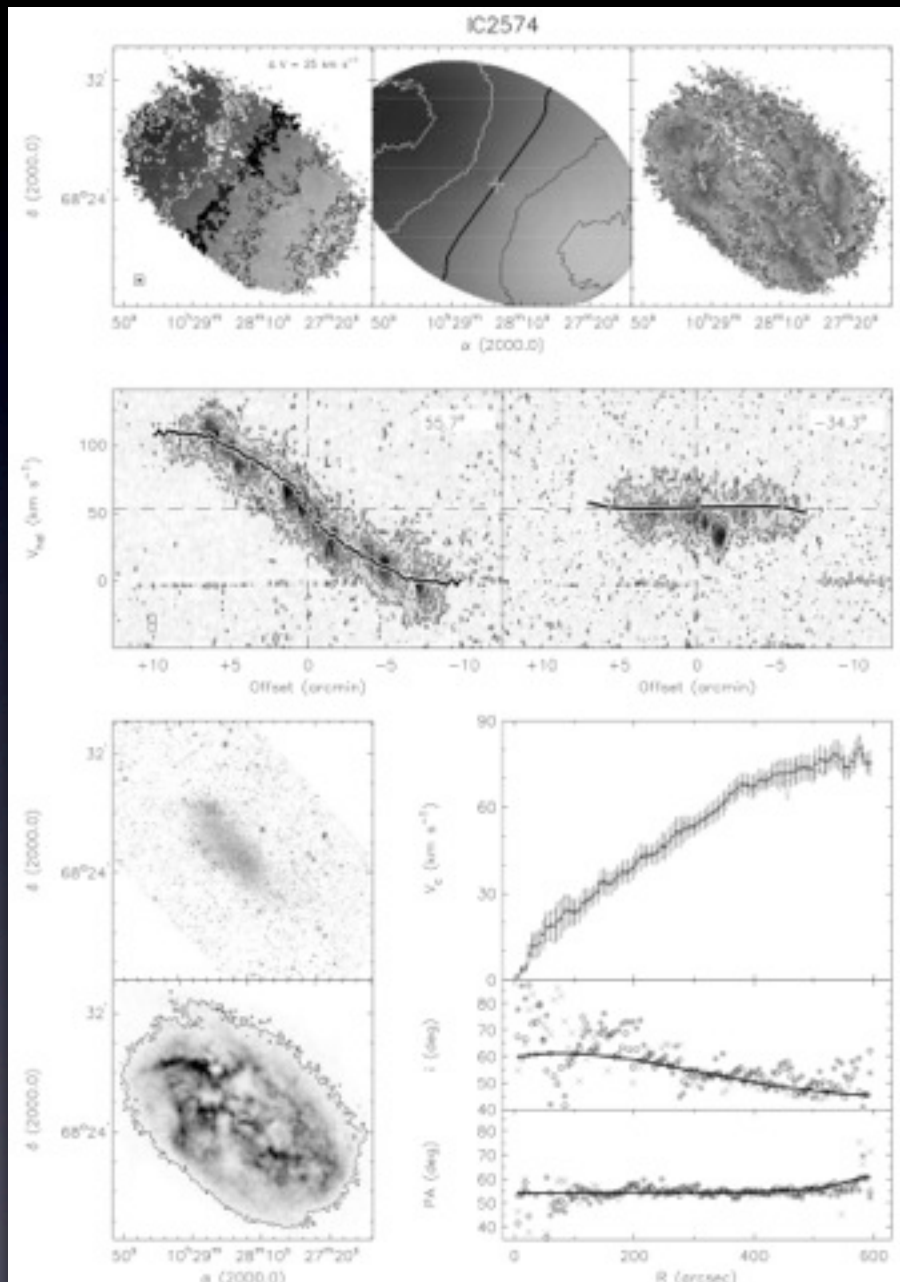

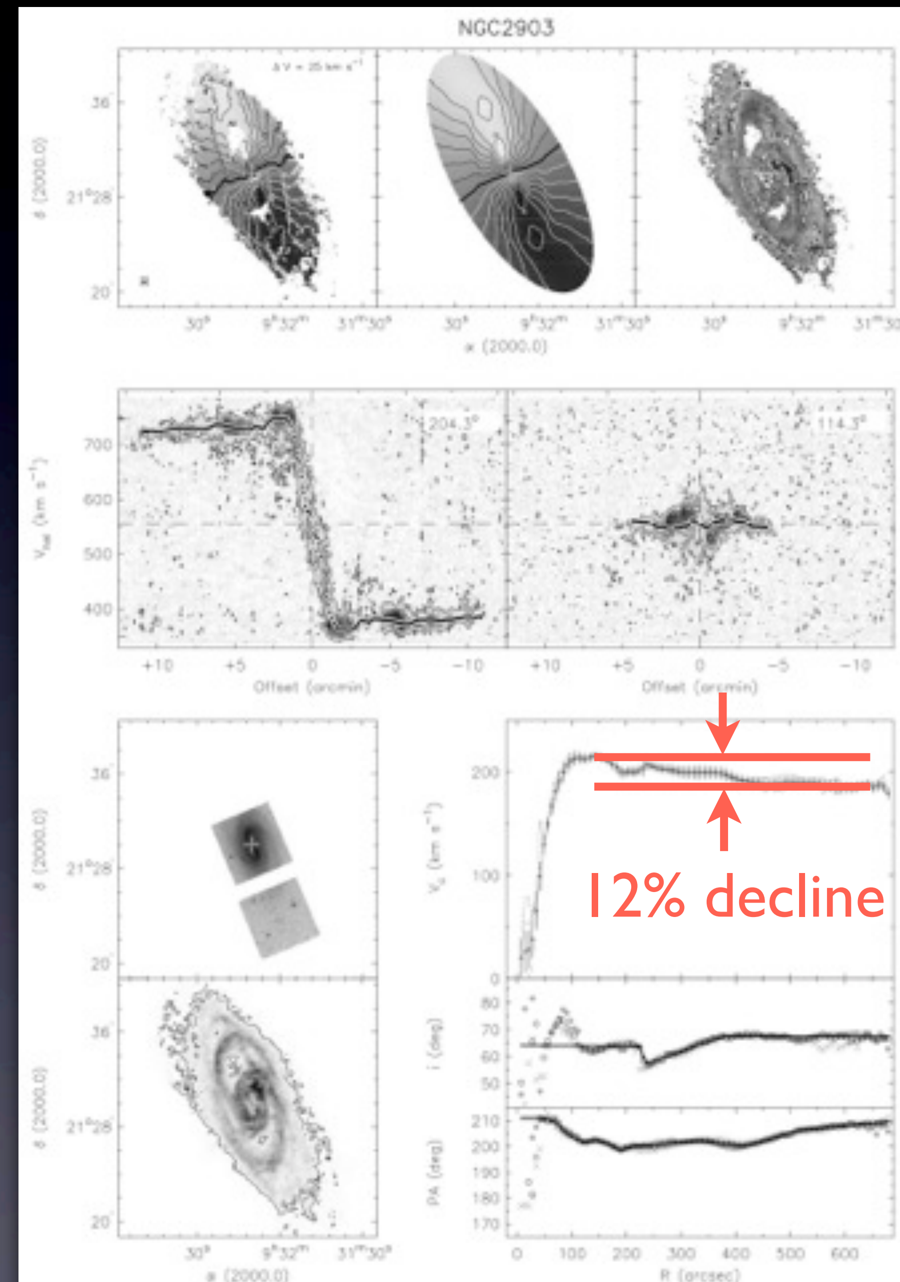

de Blok+ (2008)

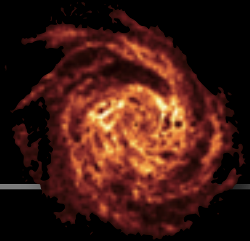

21cm spectral-line imaging - THINGS

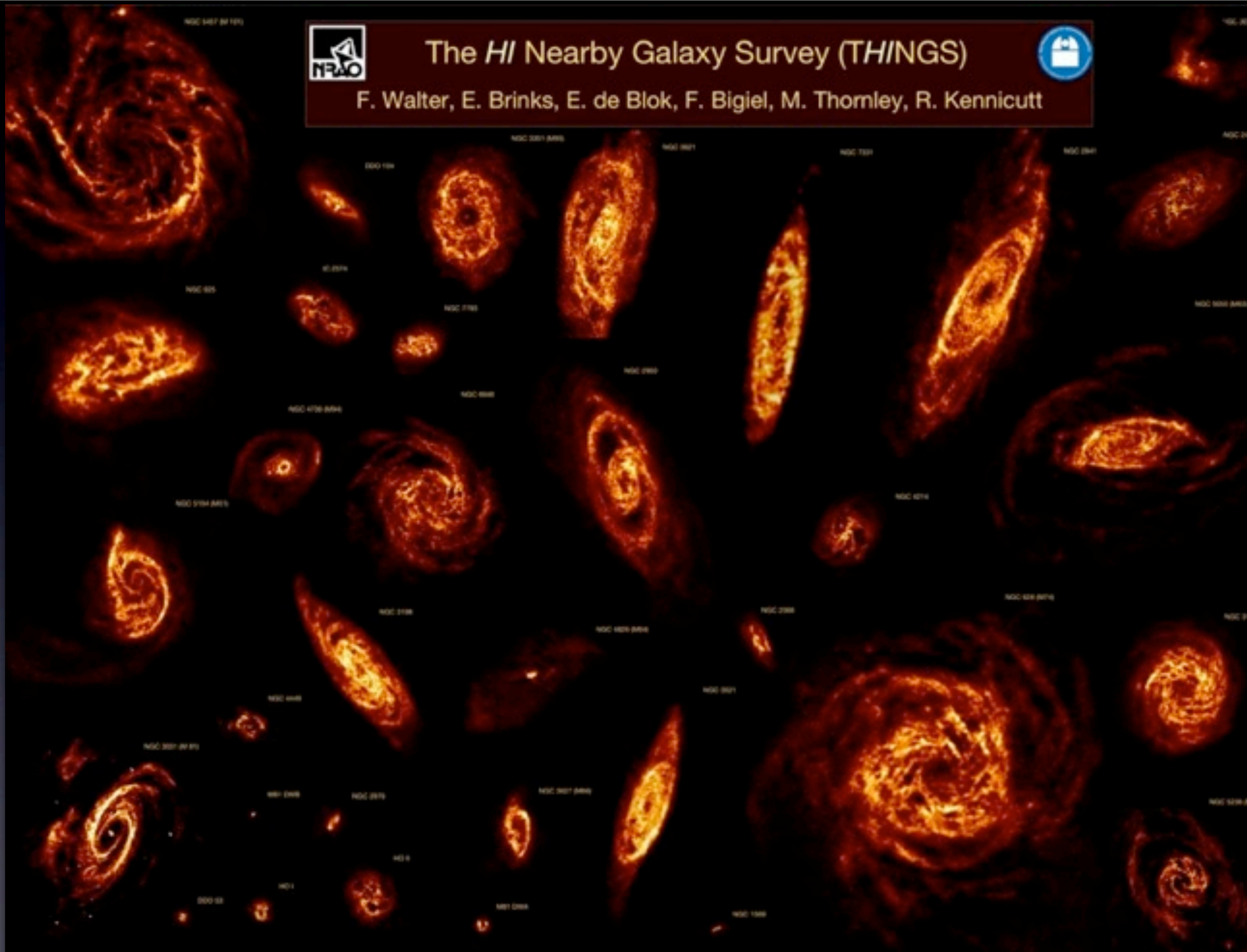

de Blok+ (2008)

21cm spectral-line imaging - perturbed disks

perturbed velocity fields

bars, warps, lopsided kinematics, interactions

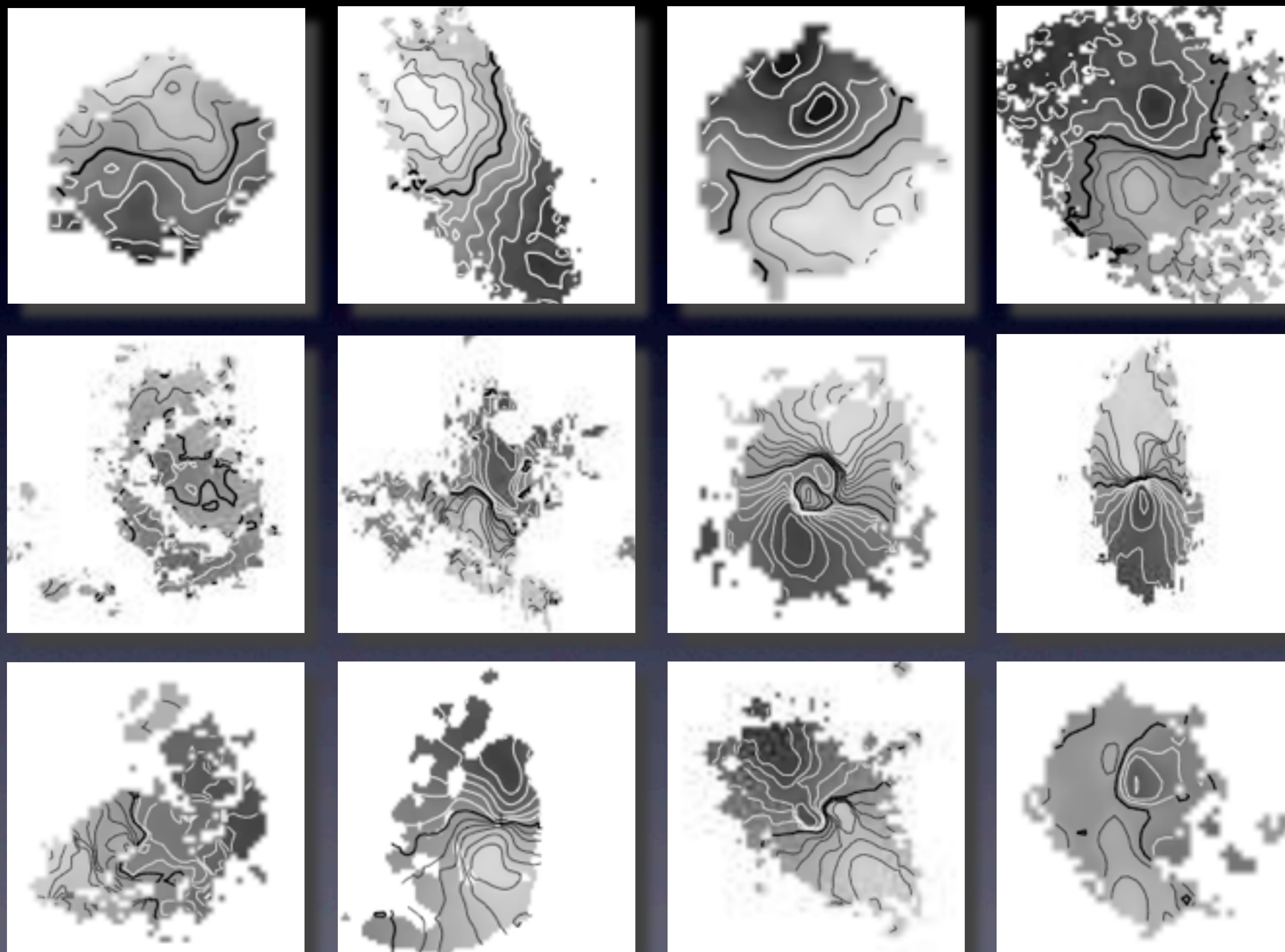

HI scaling relations

HI to optical diameters (UMa)

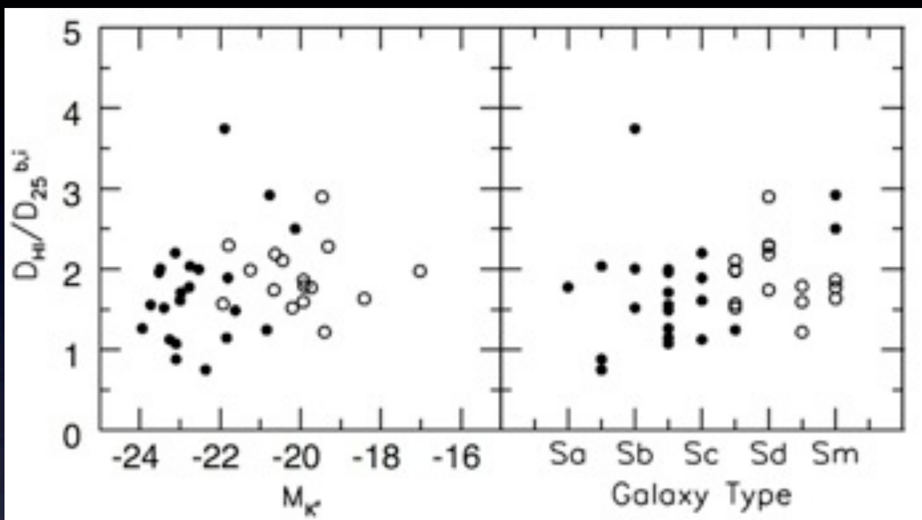

Verheijen & Sancisi '01

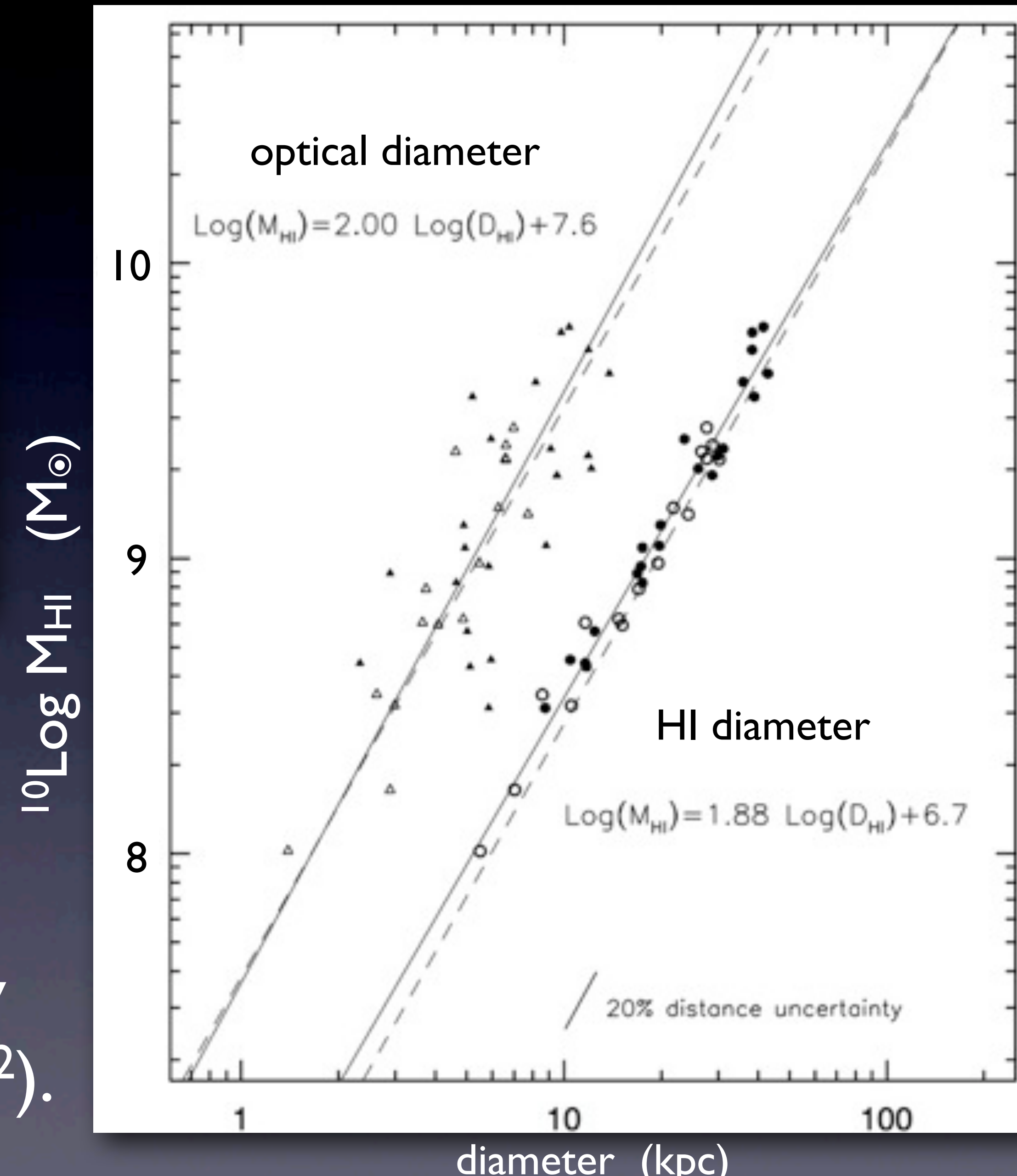

Although $<N_{HI}>$ within D_{25} varies significantly, it is nearly invariant within D_{HI} (1 $M_\odot pc^{-2}$).

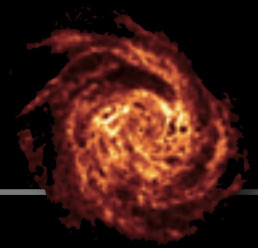

HI science topics

- Galactic and galaxy structure & kinematics.
  - the ISM, warps, lopsidedness, rotation curves, angular momentum, non-circular motions...
- Accretion and depletion of gas onto galaxies.
  - minor mergers, cold accretion, ram-pressure stripping, outflows and feedback...
- Formation of galaxies and large scale structure.
  - HIMF, major mergers, spin alignments, void population, cosmic web, TF distances...
- Cosmic evolution of gas in galaxies.
  - $\Omega_{HI}(z)$, gas fractions vs mass, role of gas in downsizing...

slopes of outer rotation curves

slope between 2 h_{disk} and the last measured point

$$S_{2h,lmp} = \frac{\mathrm{Log}(V_{2h} / V_{lmp})}{\mathrm{Log}(R_{2h} / R_{lmp})}$$

S>0 : rising

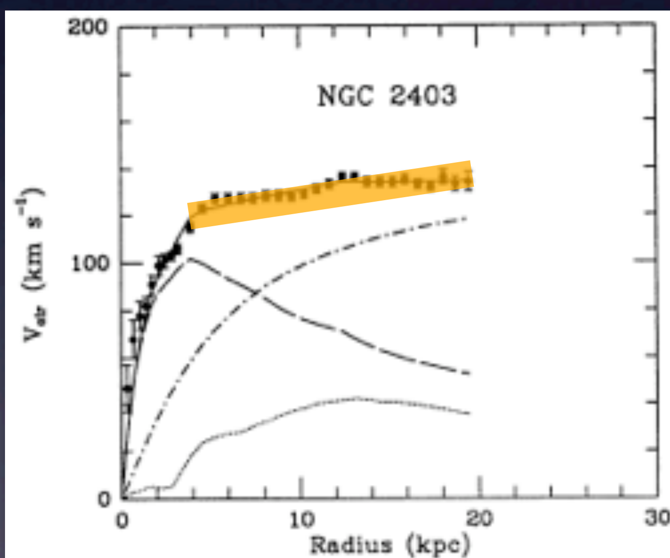

S=0 : flat

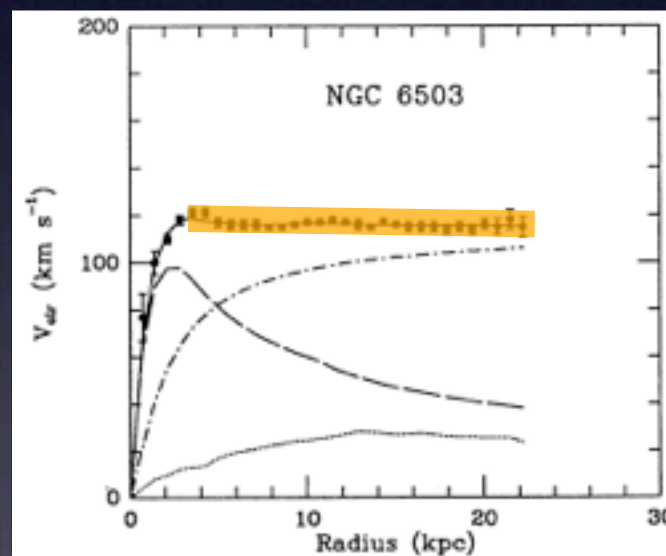

S<0 : declining

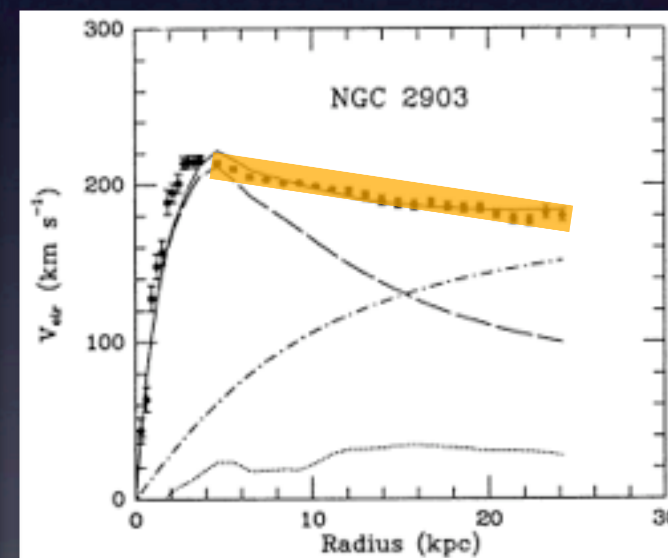

Begeman et al (1991)

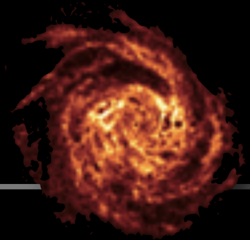

slopes of outer rotation curves

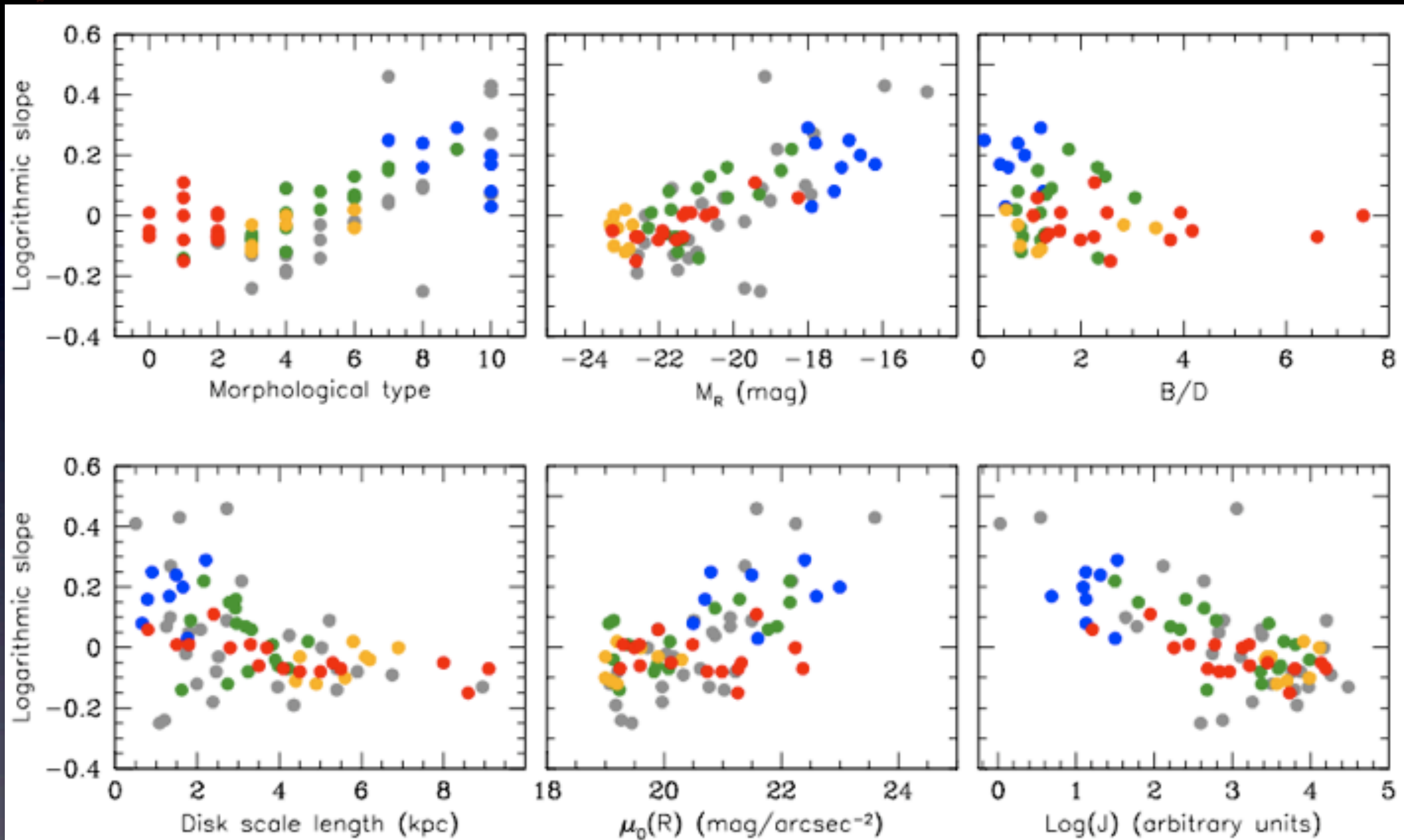

Casertano & van Gorkom

Verheijen & Sancisi

Noordermeer et al

Swaters et al

Spekkens & Giovanelli

Rotation curves and the Tully-Fisher relation

rising flat declining

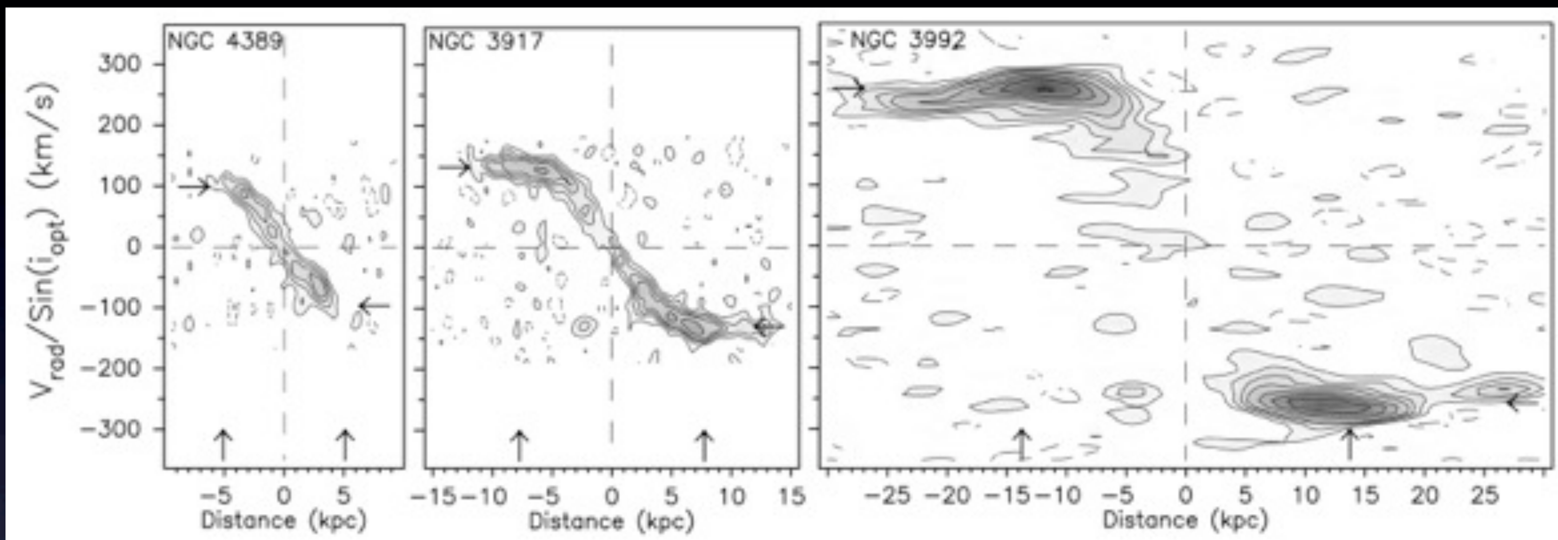

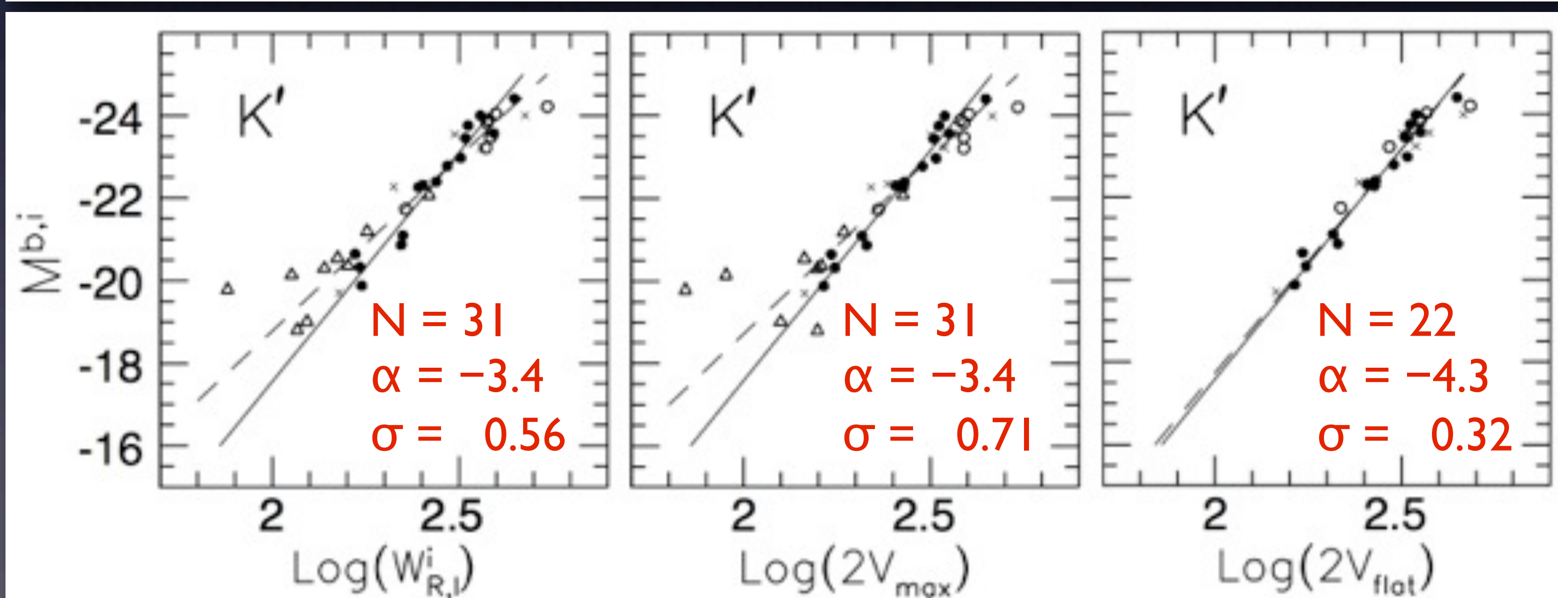

Verheijen '01

W_{20} V_{max} V_{flat}

Rotation curves *beyond the optical radius* (R_{25}) provide the relevant kinematic measure.

Extent of Hα rotation curves is insufficient to measure V_{flat} consistently.

MV01

Oosterloo et al 2007

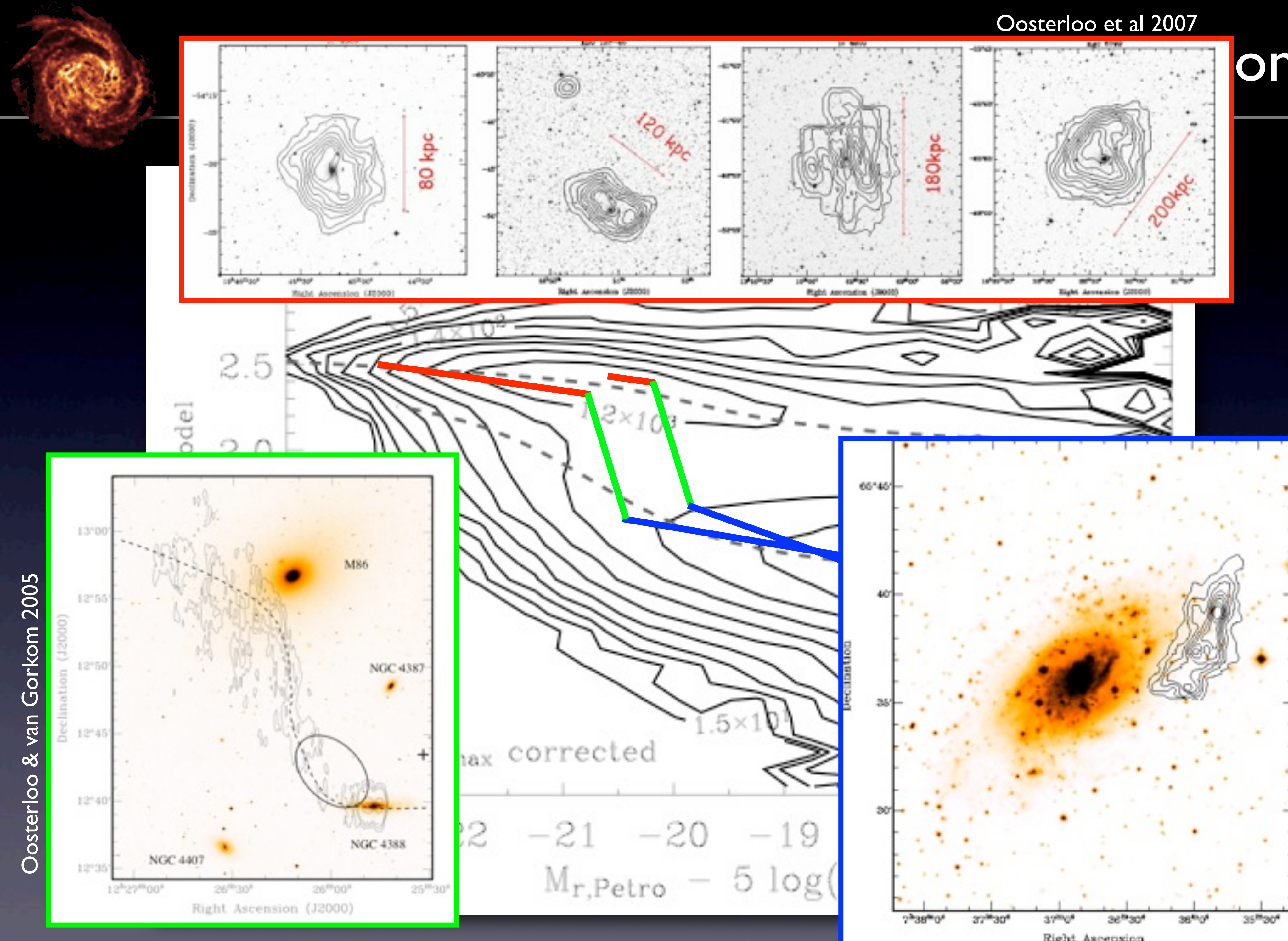

Oosterloo & van Gorkom 2005

Fraternali et al 2002

Fueling the Blue Cloud

25% of galaxies undergo minor mergers

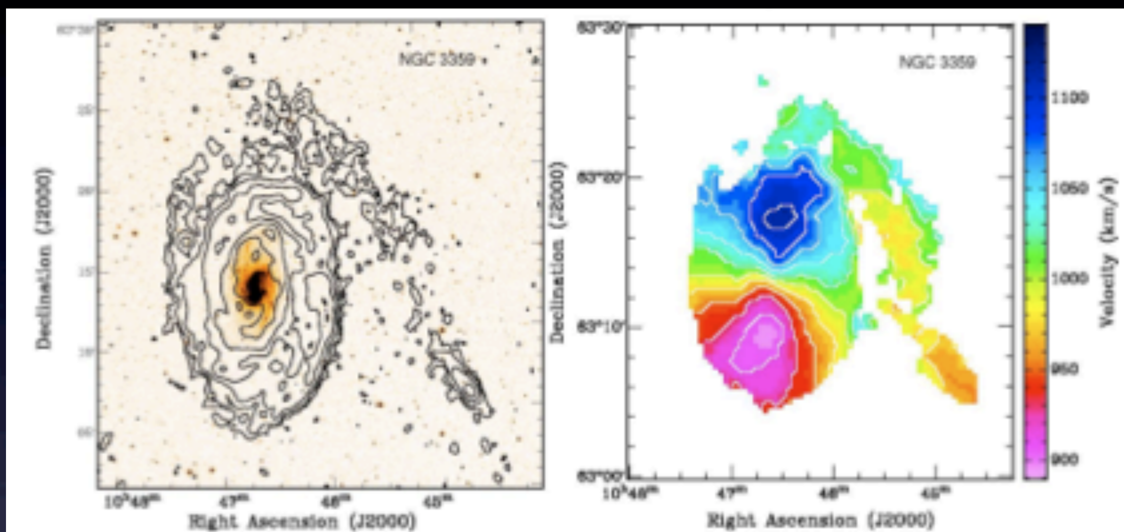

Sancisi+ A&A Rev. 2008

sustaining star formation

-

building up stellar mass

Evidence for cold accretion

or

Galactic Fountain / Fallback?

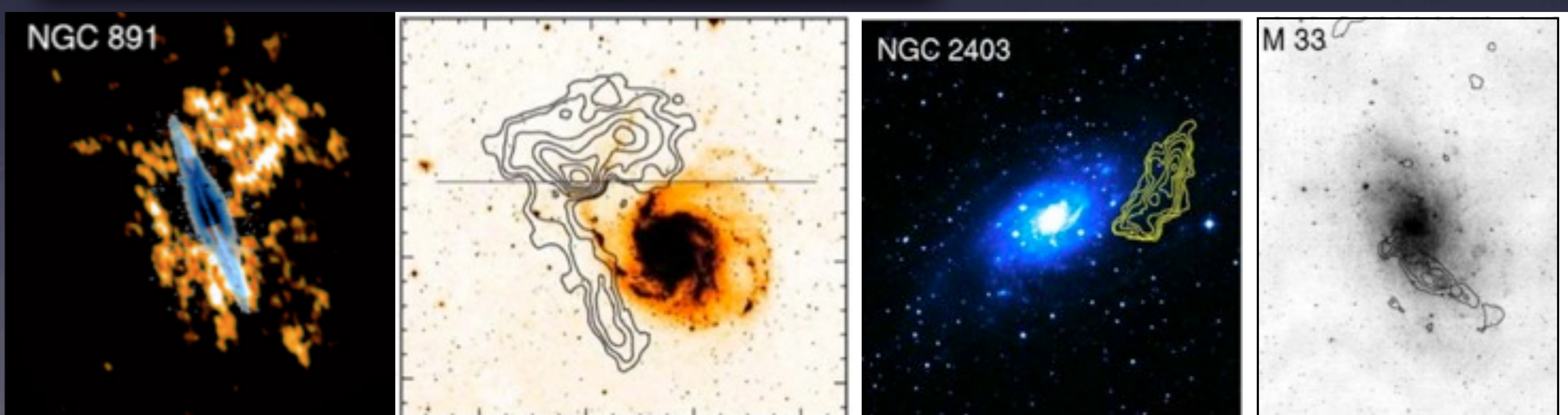

Oosterloo+ 2007

Warps and stellar streams

Is there a link?

NGC 5055

R. Jay GaBany

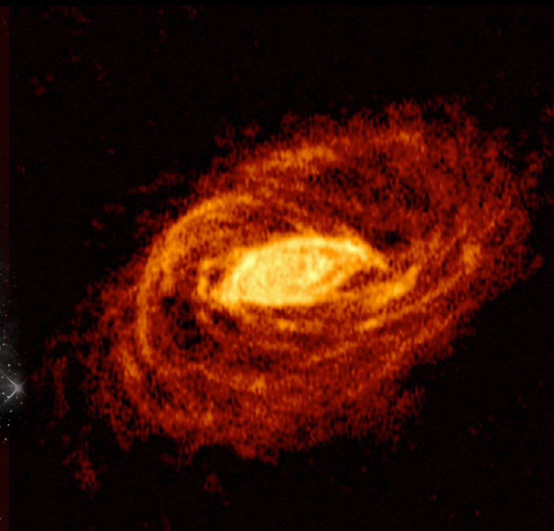

Battaglia+ 05

NGC 5907

R. Jay GaBany

NGC 4013

R. Jay GaBany

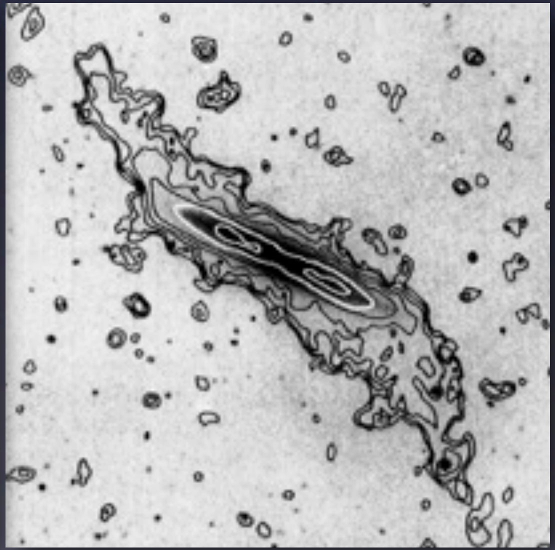

Bottema 95

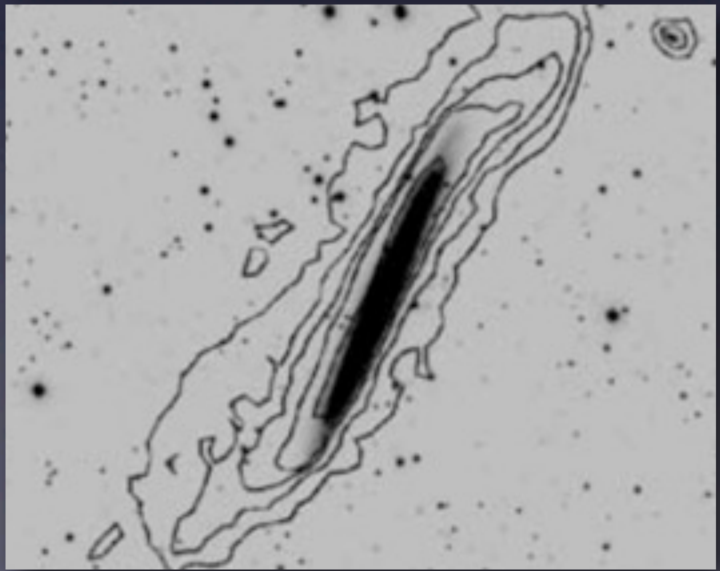

Shang+ 98

Crossing the Green Valley

gas-stripping in the Virgo cluster

NGC 4522 VLA

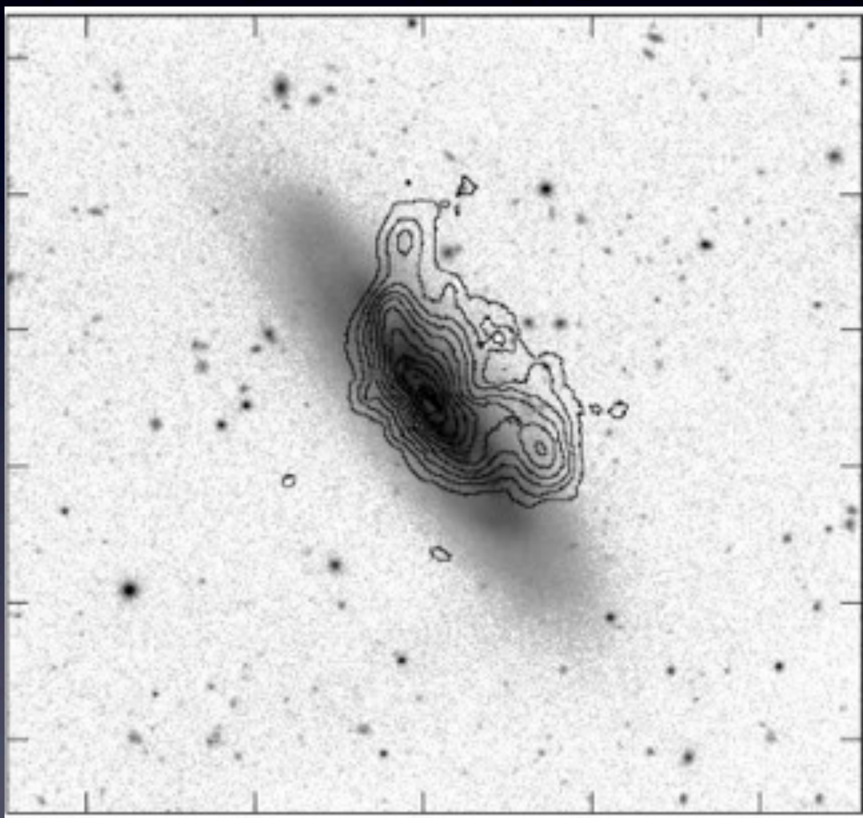

Kenney et al, 2004

Ram-pressure induced
(and truncated?) star formation

NGC 4388 WSRT

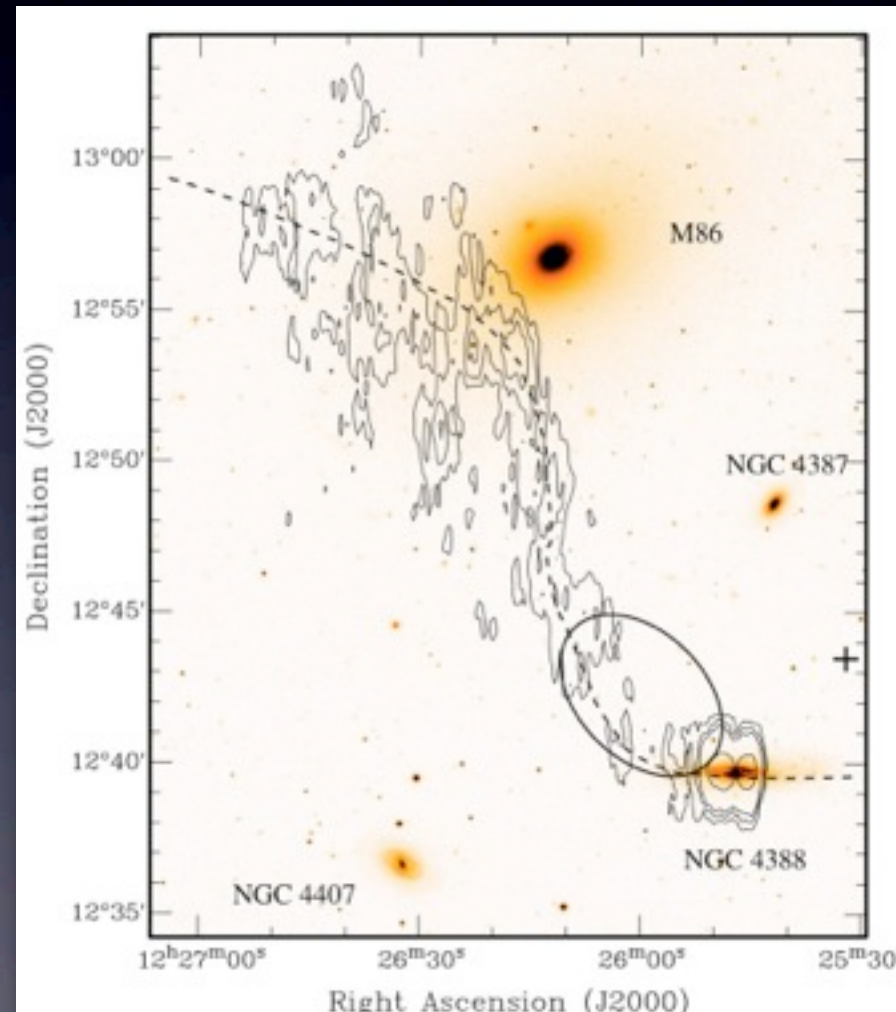

Oosterloo & van Gorkom, 2005

Passive galaxies on the Red Sequence ?

Atlas^{3D} : HI imaging of 166 early-types

1/3 detected
40% of E's in field

Lower density regions : extended and regular HI disk

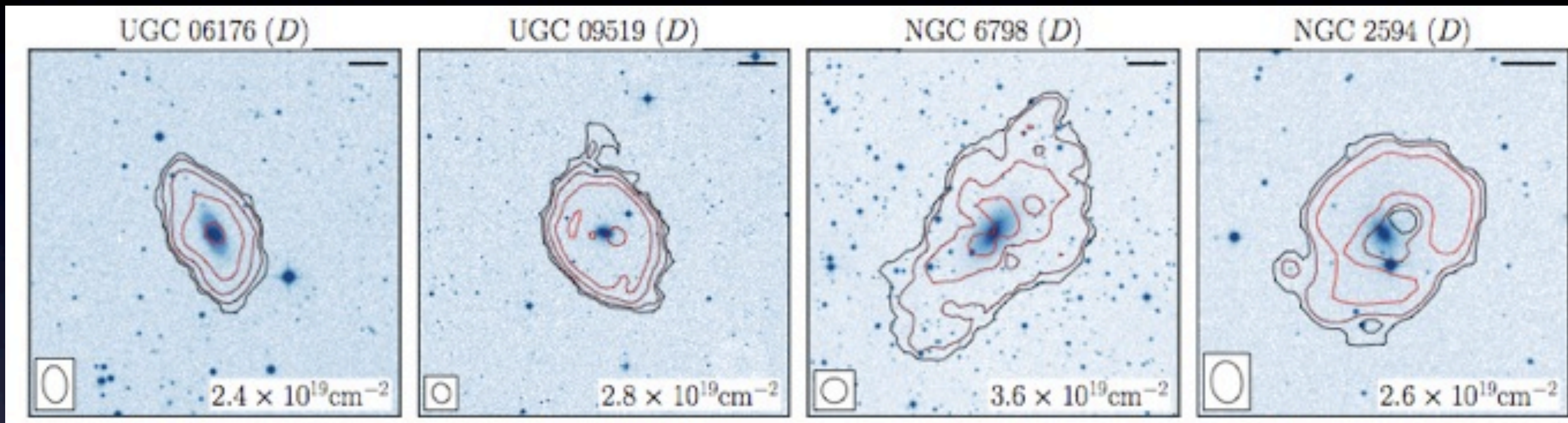

Higher density regions : clumpy and unstructured

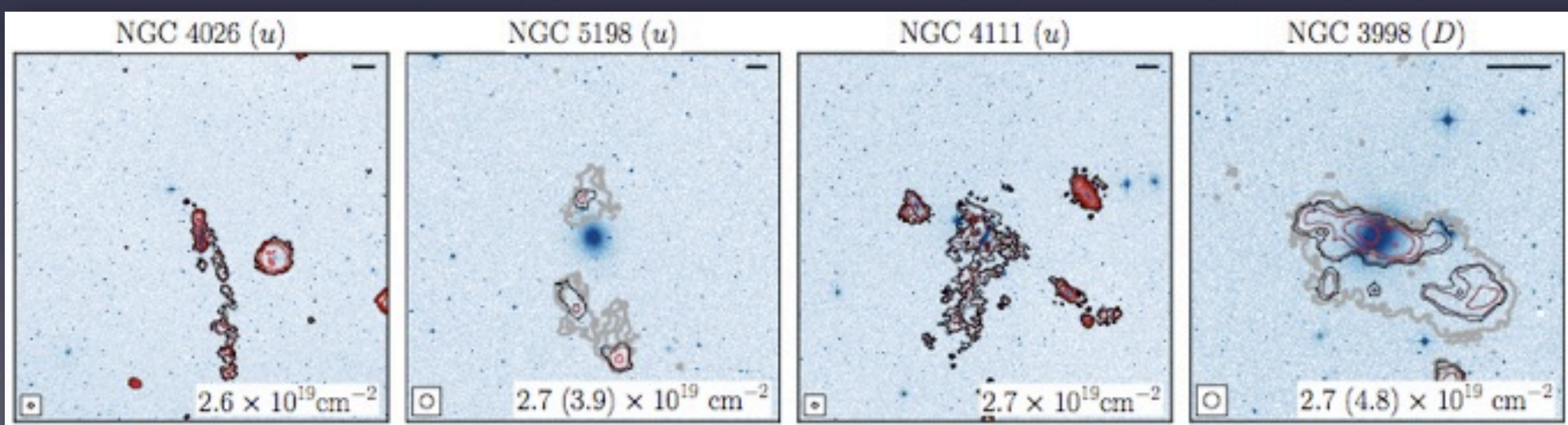

Serra et al. 2011

Environmental dependence of gas content

Virgo | **Ursa Major**

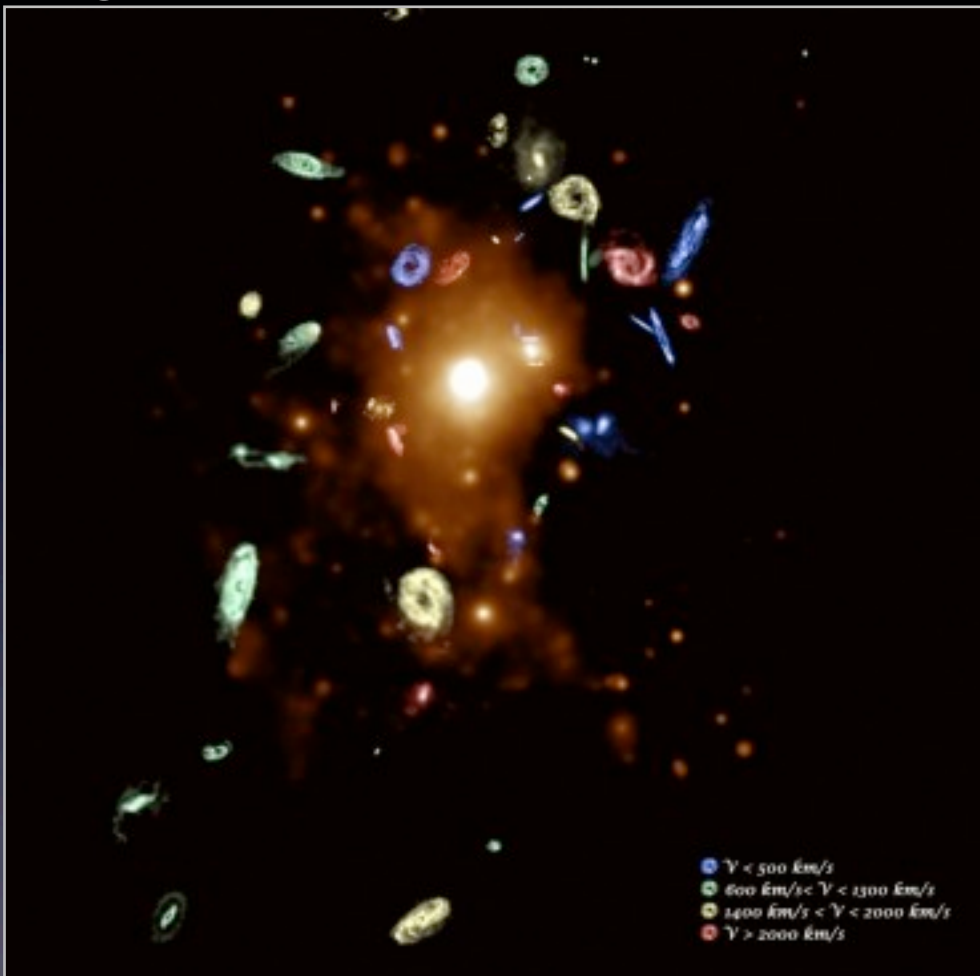

Chung et al 2009 — Very Large Array

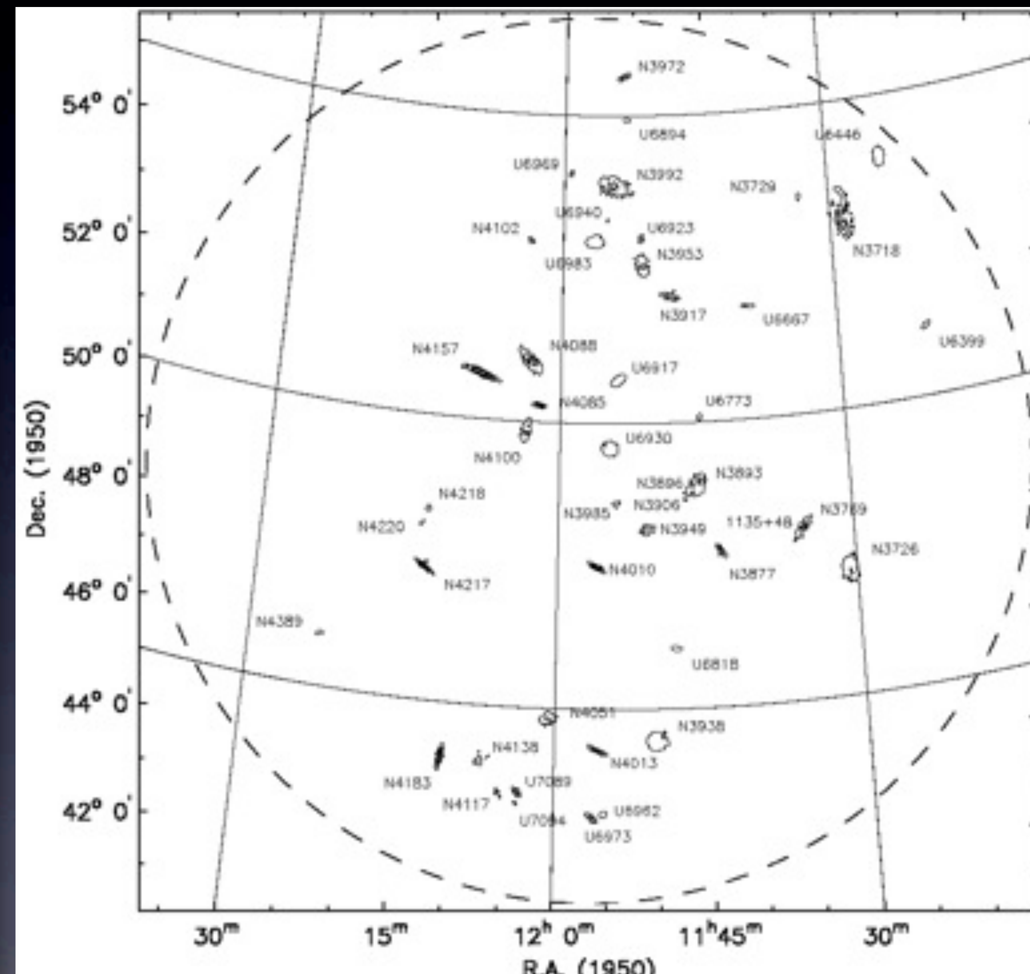

Verheijen & Sancisi 2001 — Westerbork

VIVA : VLA Imaging of Virgo galaxies in Atomic gas

HI, ICM, SFR, SP interrelations

Coma

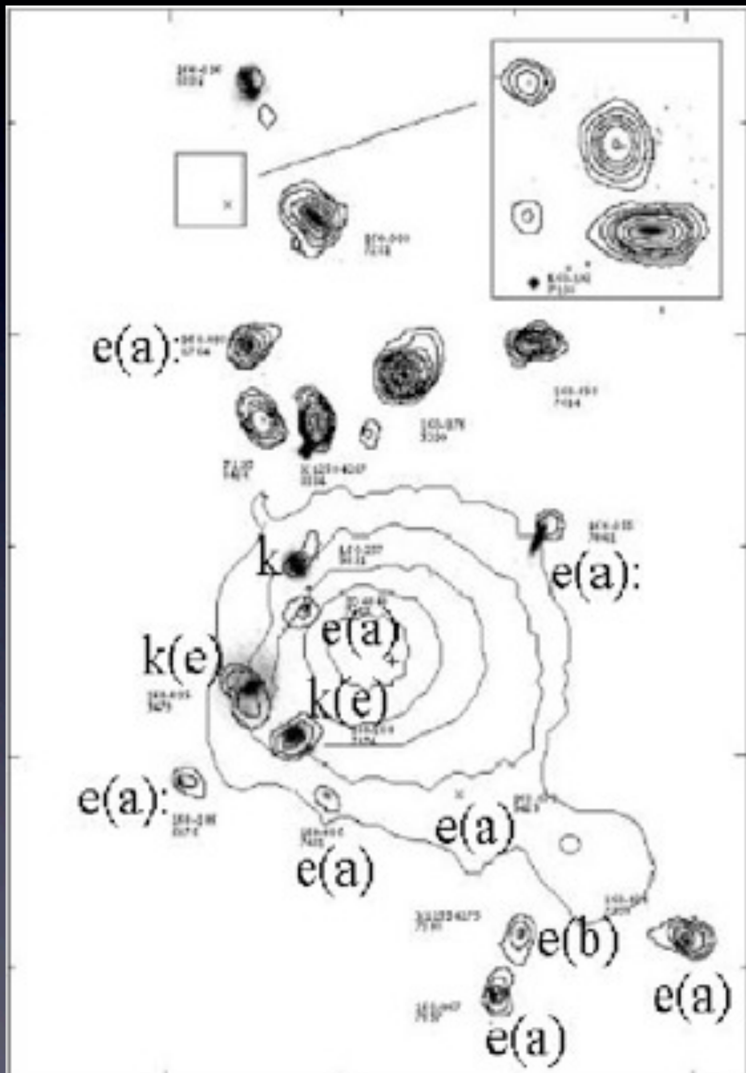

Bravo-Alfaro+ 01

Abell 2670

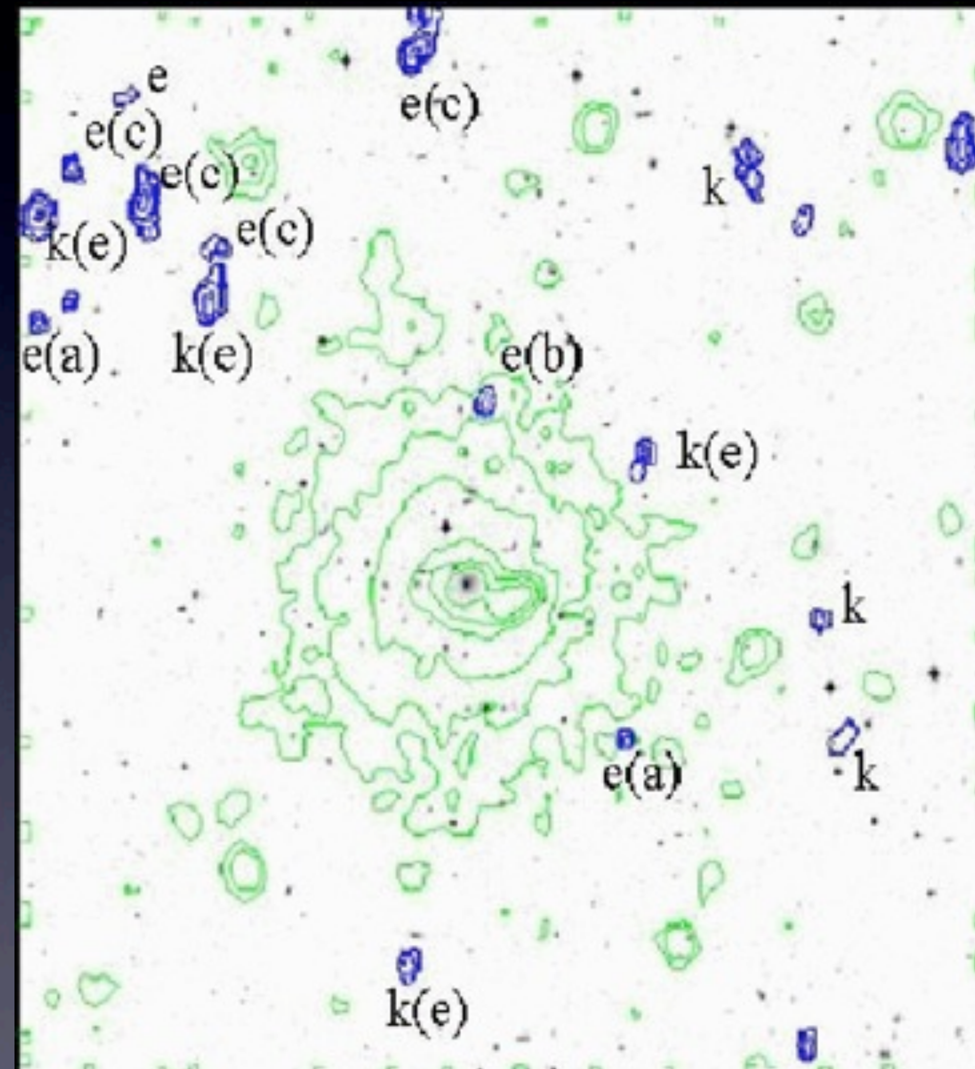

Poggianti & van Gorkom, 01

Void Galaxy Survey

Kreckel+ 11

A pilot study of 15 void galaxies.

4/15 are strongly perturbed

Void galaxies seem to be gas-rich with evidence for ongoing gas accretion, major & minor interactions, and alignment along cosmic filaments.

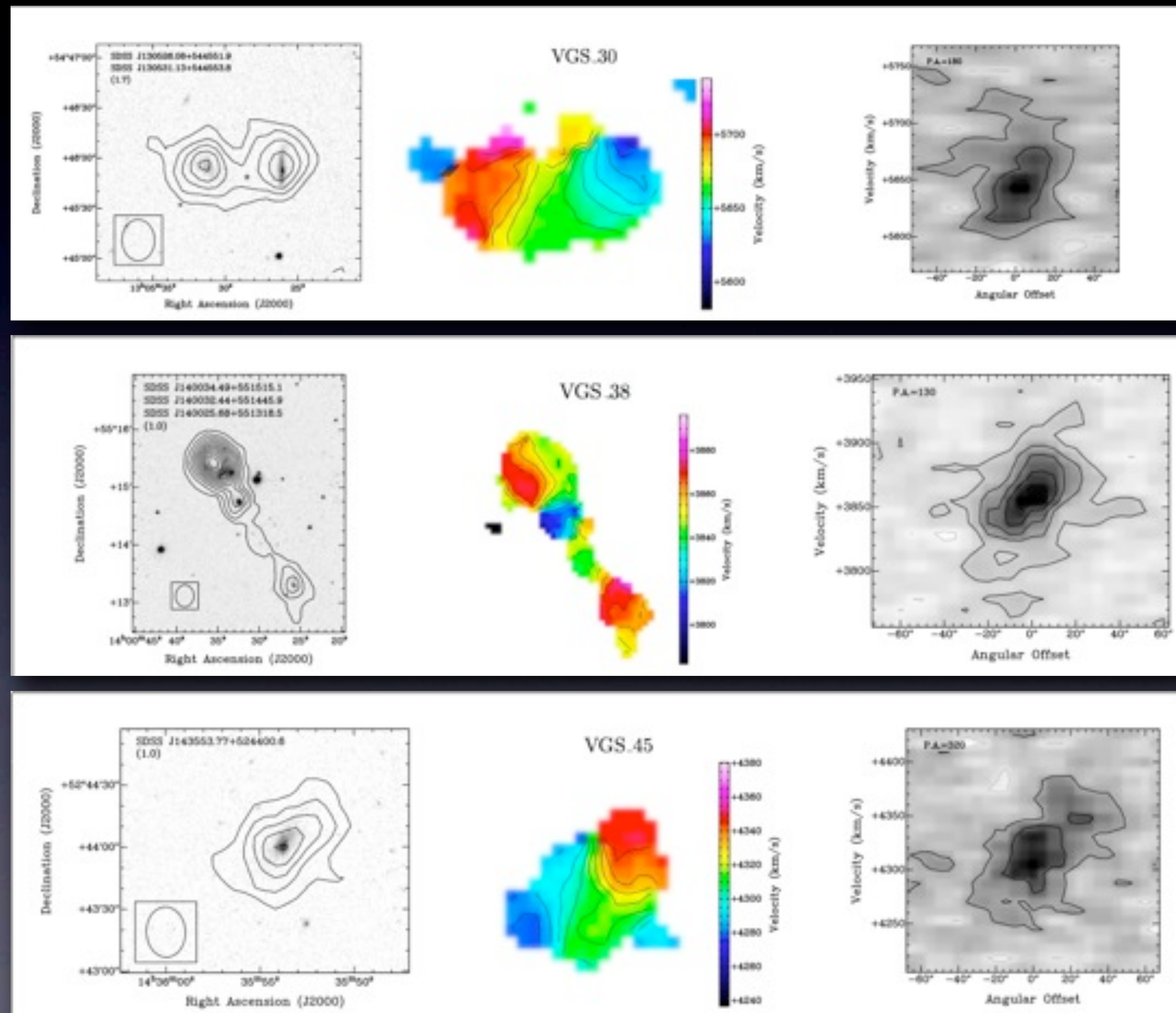

accretion and depletion of gas

beam = 30”x30” beam = 45”x45” beam = 18”x90”

Fraternali et al

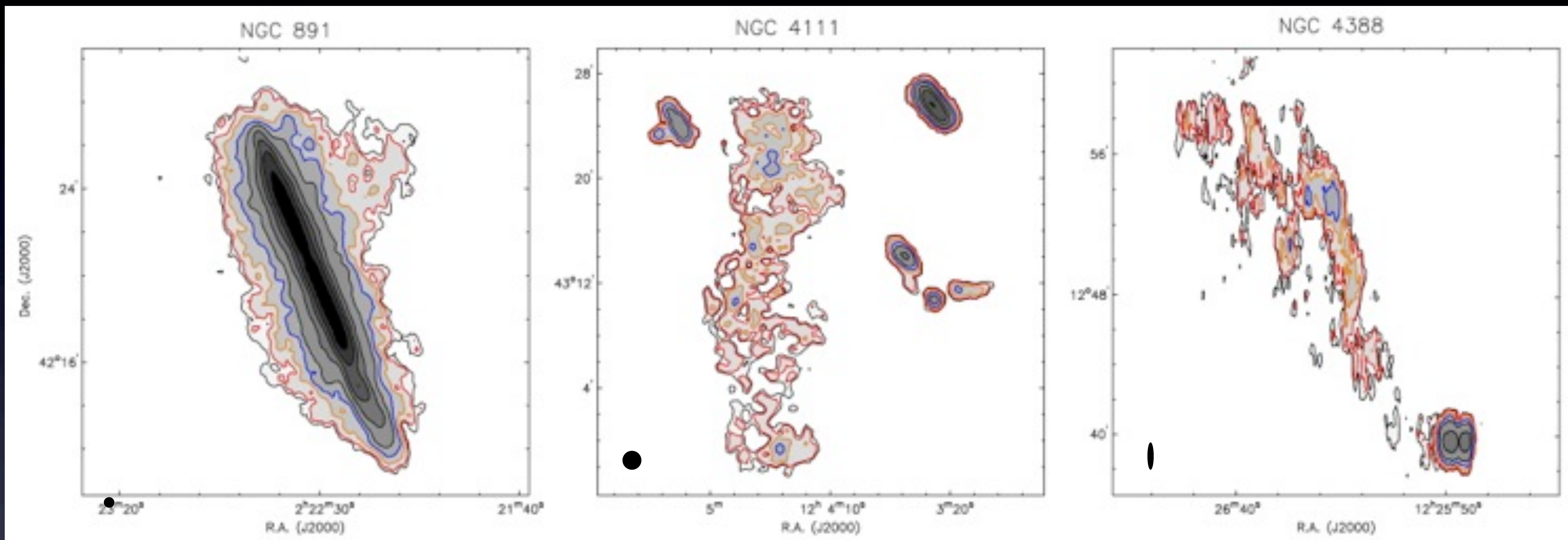

Oosterloo et al

Verheijen et al

Map and measure these filaments
in various evironments at different redshifts.

$2x10^{19}$ (atoms/cm^2)
$5x10^{19}$ (atoms/cm^2)
$10x10^{19}$ (atoms/cm^2)

Which gas depletion mechanisms dominate where?

Coming soon : all-sky blind HI imaging surveys

Blind
VLA-D survey
of Ursa Major

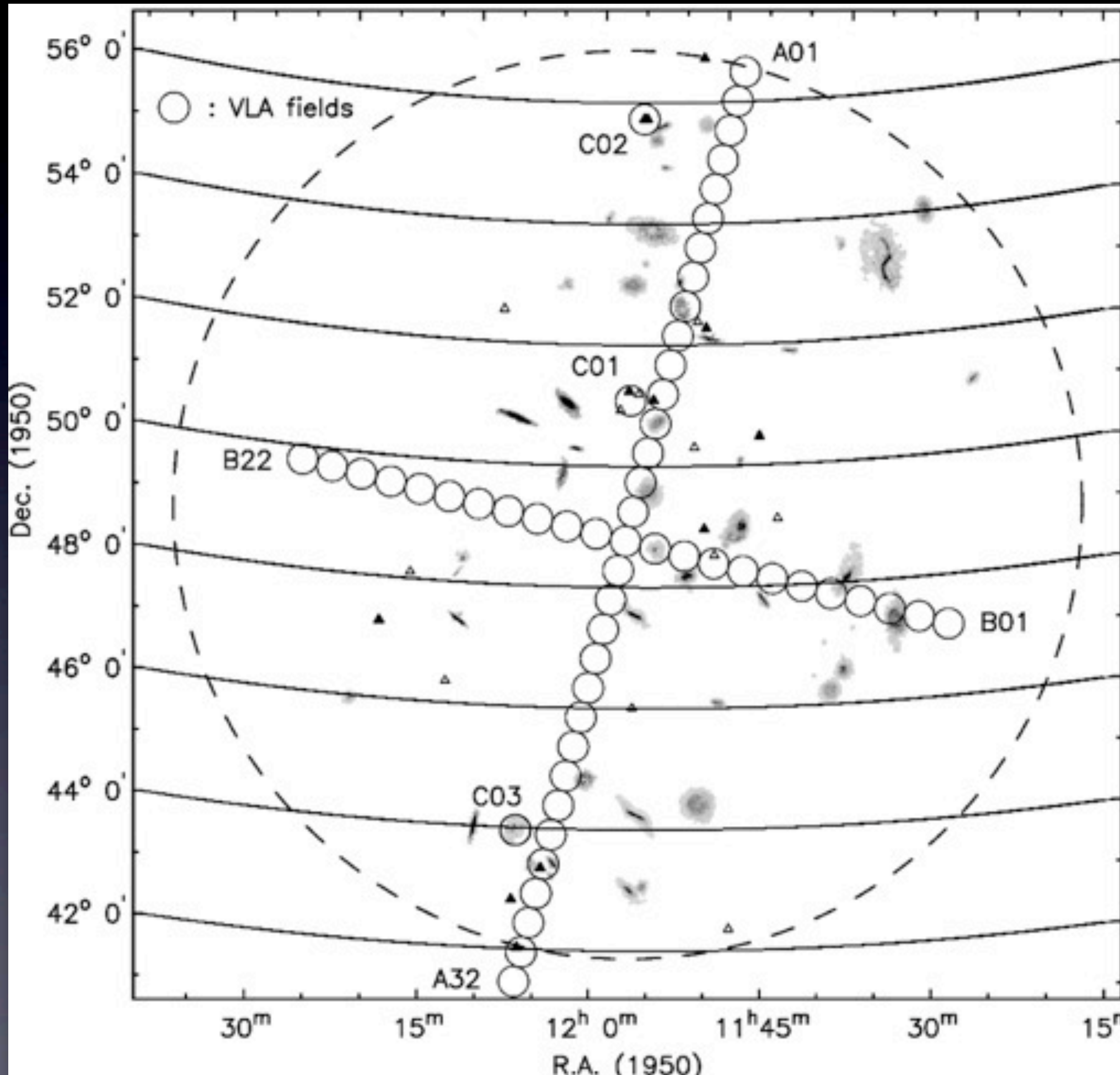

Coming soon : all-sky blind HI imaging surveys

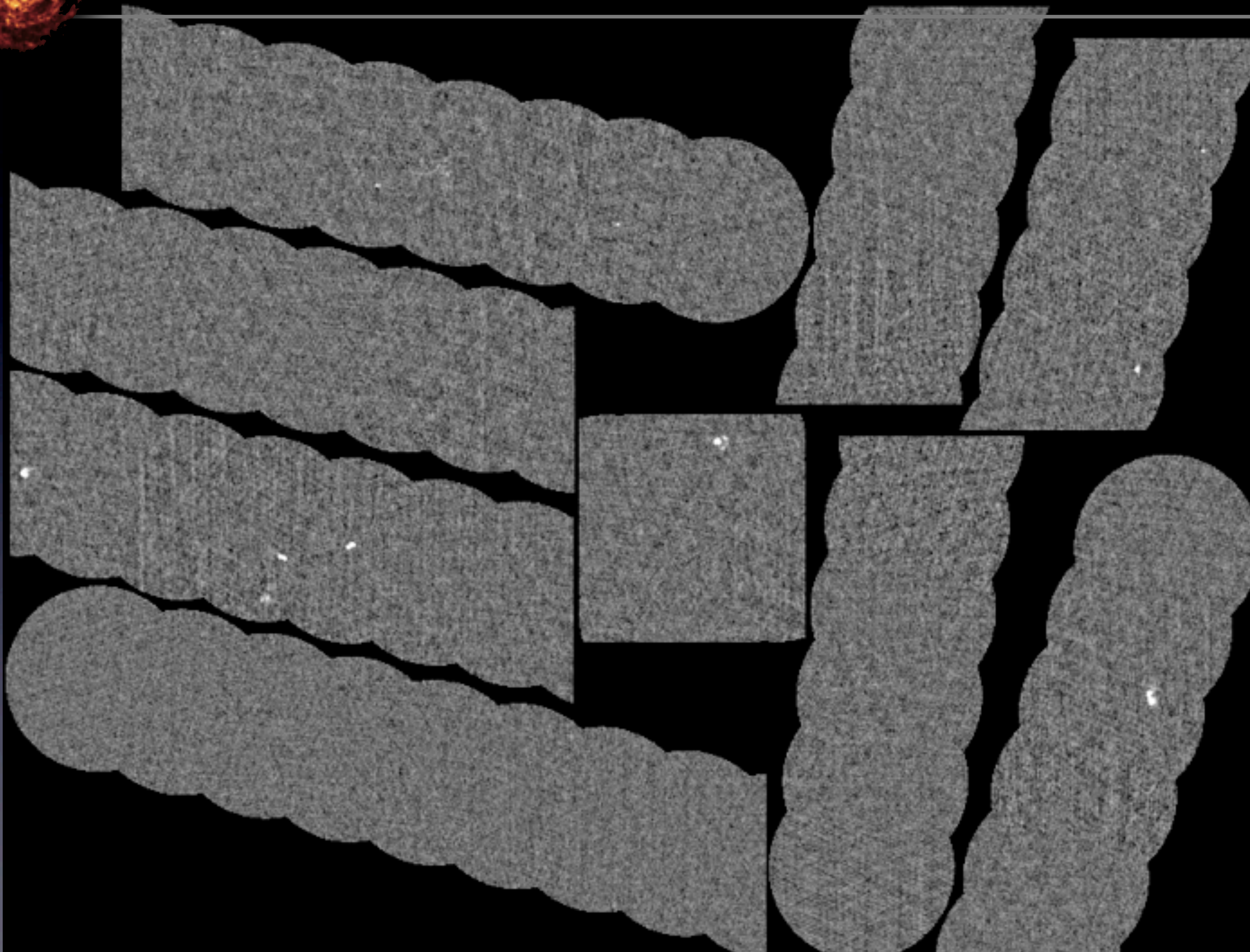

Dwingeloo

The push to higher redshifts

WSRT ultra-deep HI survey of galaxy clusters at z=0.2

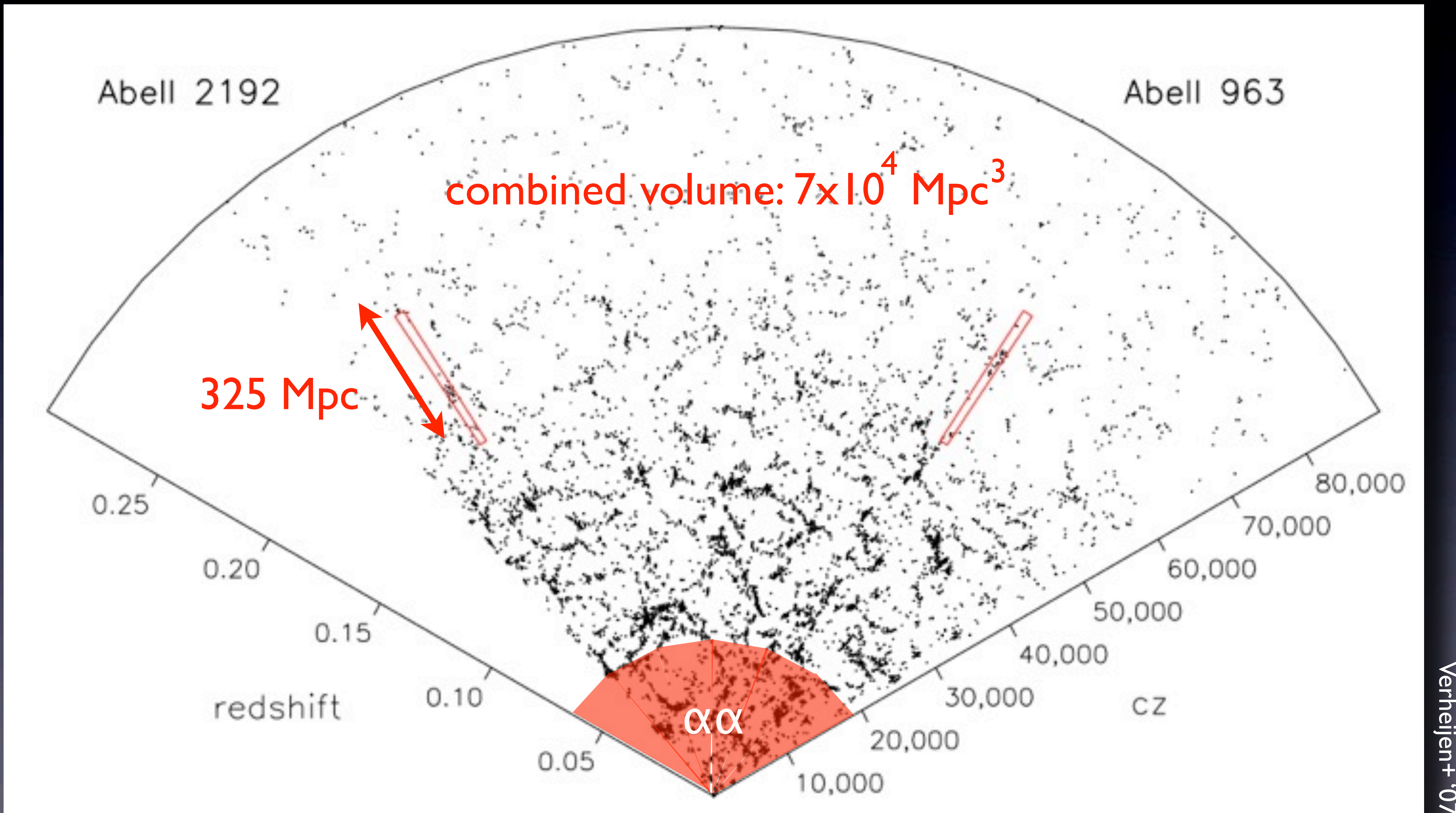

SDSS redshift cone

The push to higher redshifts

Verheijen+, in prep

Abell 2192

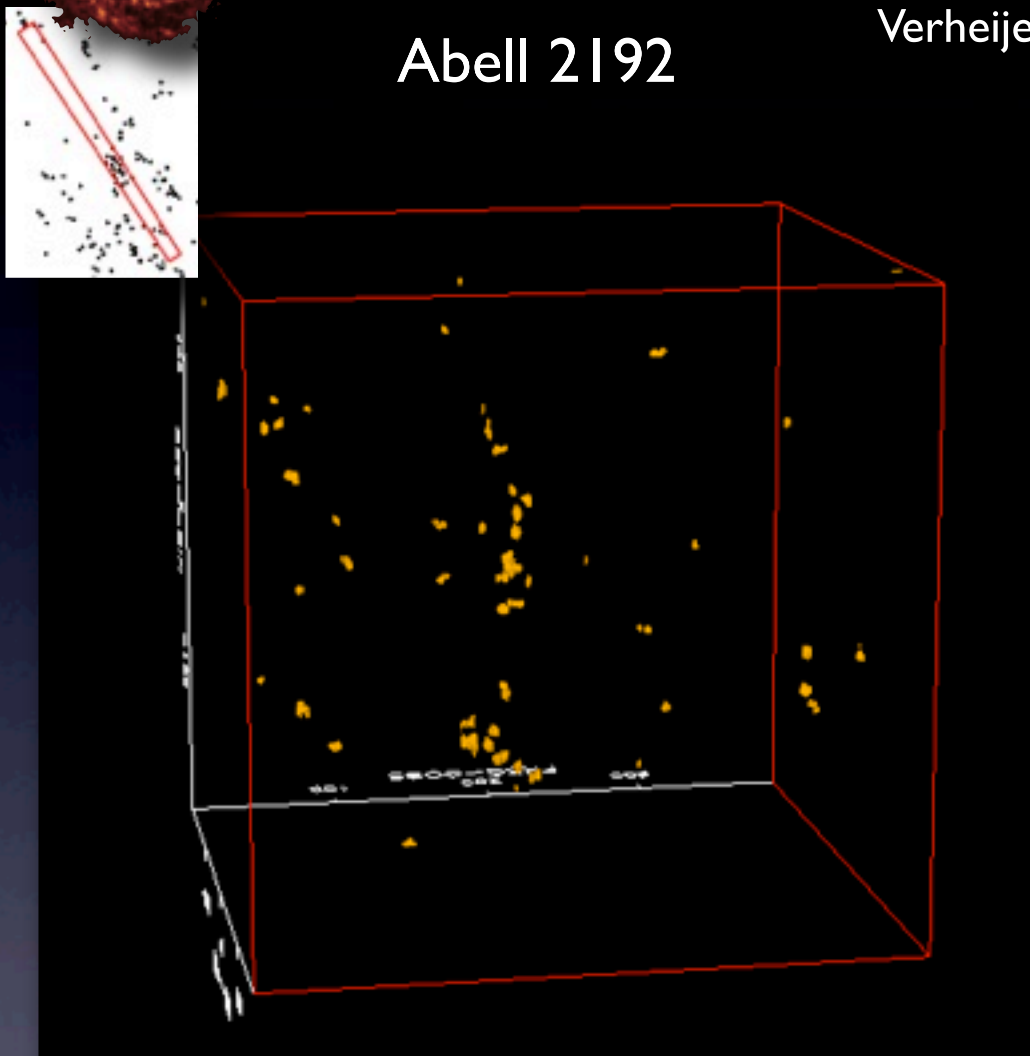

Abell 963

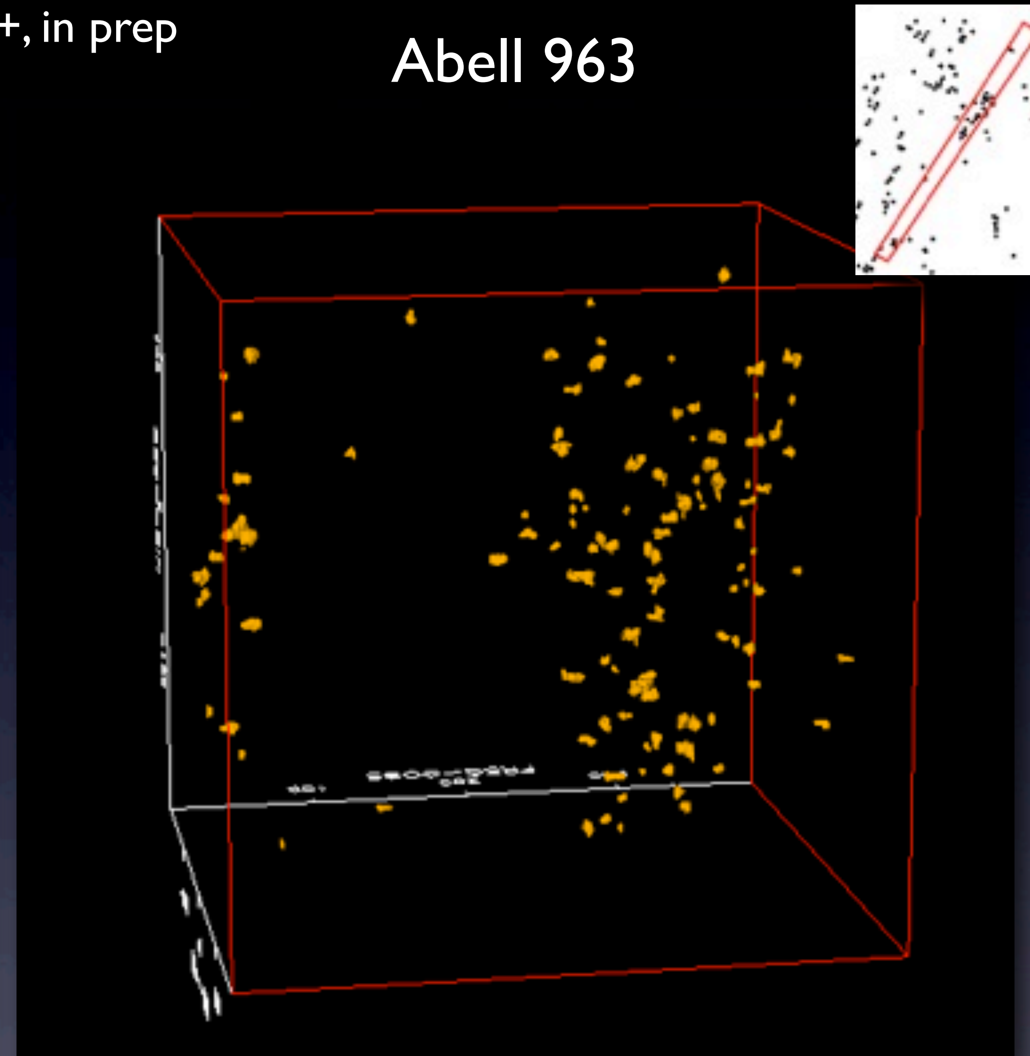

Cube size : 9.5 x 9.5 x 325 Mpc^3
Beam size : 65 x 80 kpc^2 x 80 km/s

Are Butcher-Oemler clusters accreting a more gas-rich field population?

The push to higher redshifts

Colour-Magnitude diagram

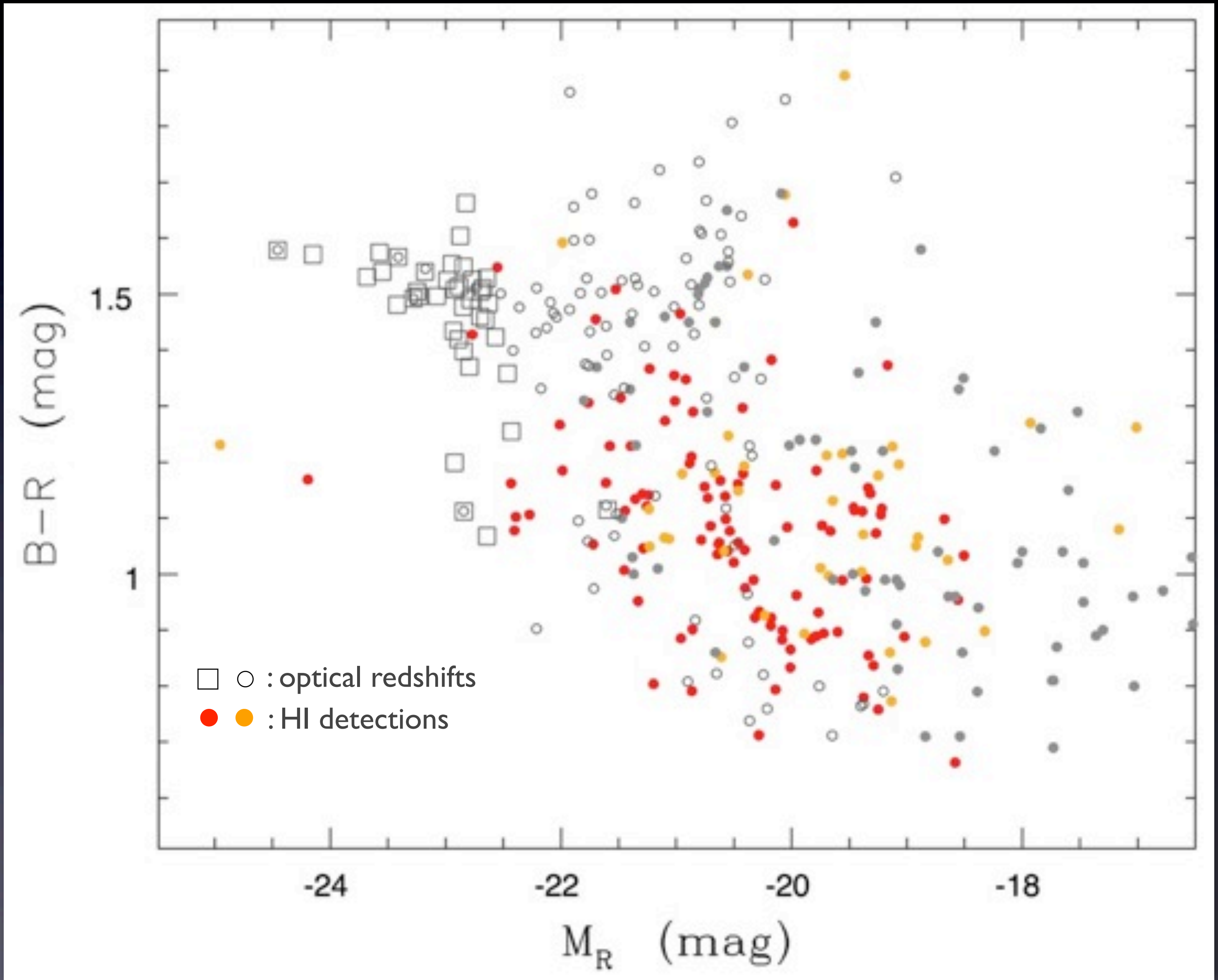

Verheijen+, in prep

The push to higher redshifts

Stacking HI spectra (based on pilot data)

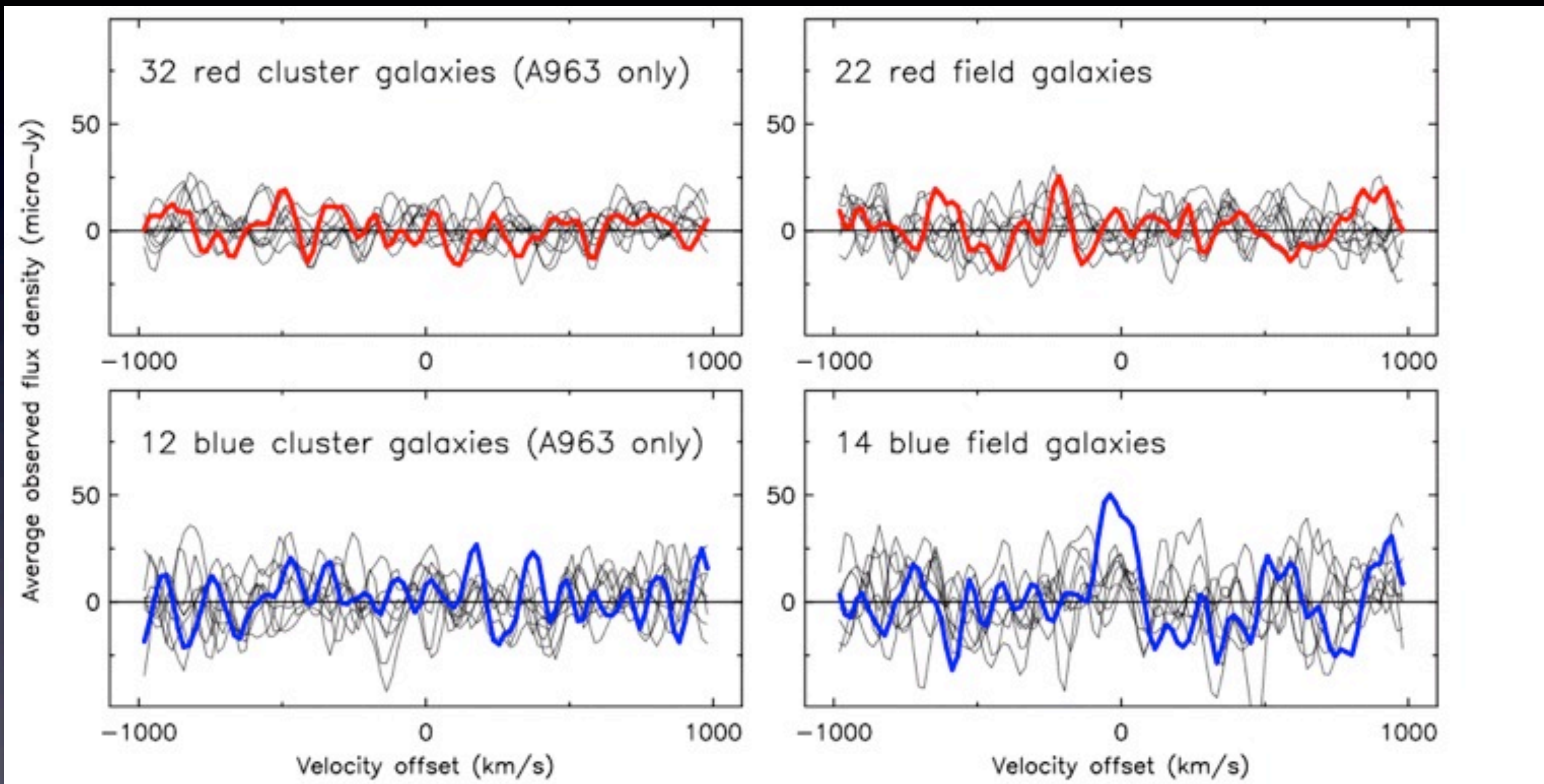

Verheijen+ '07

Average HI mass ≈ $2 \times 10^9 \, M_\odot$

HI absorption line studies

- Traces cold gas in (front of) bright radio sources / AGNs
- Reveals high-speed inflows and outflows (fueling & feedback)
- Observable at high redshifts

Emonts et al 2005

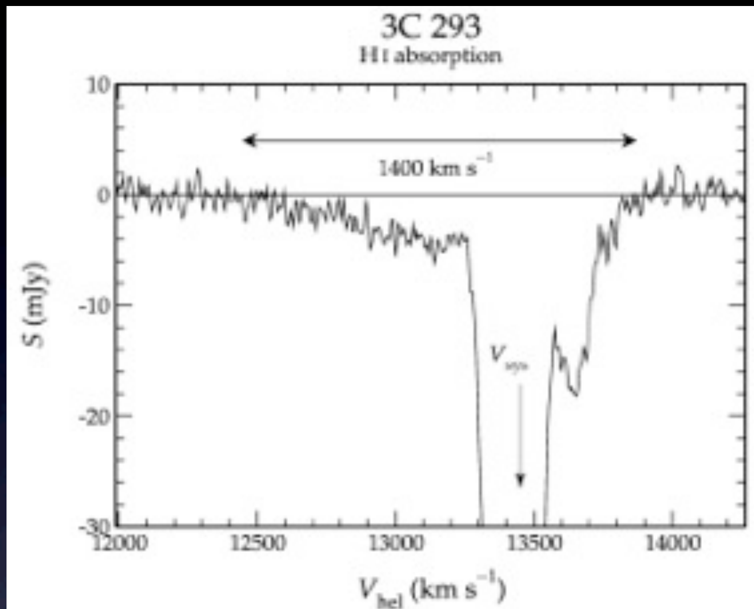

Morganti et al 2005

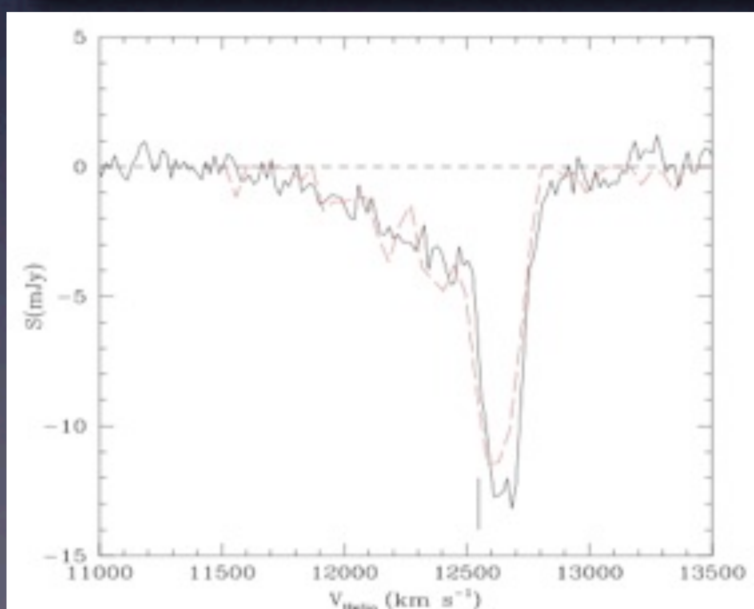

HI absorption against binary SMBH

Morganti et al 2009

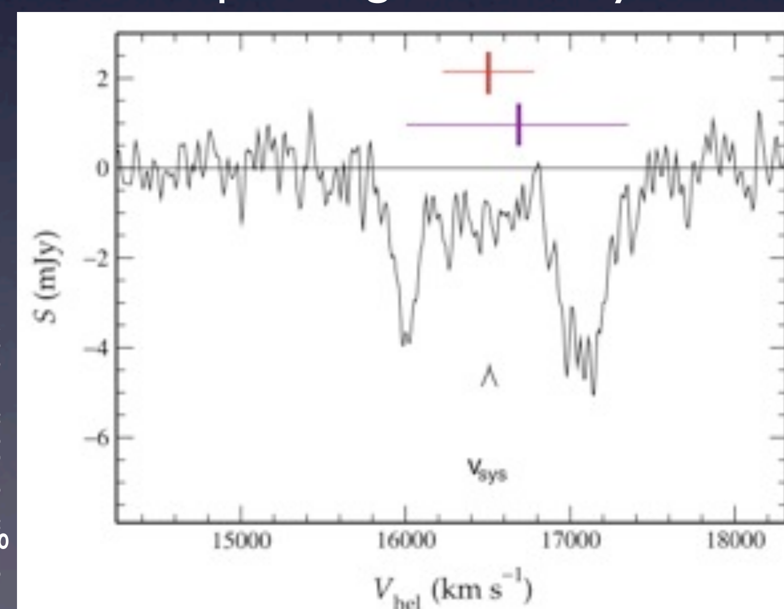

HI self-absorption

DRAO - Canadian Galactic Plane Survey

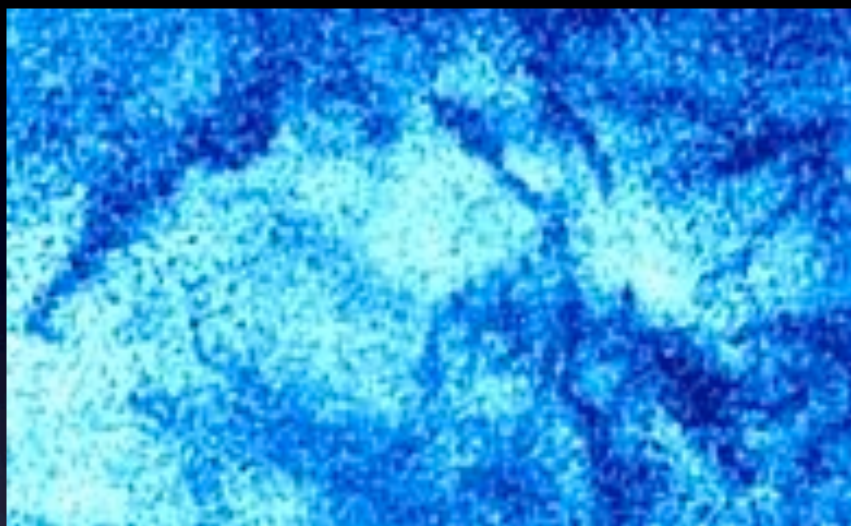

Taylor et al, 2003

VLA

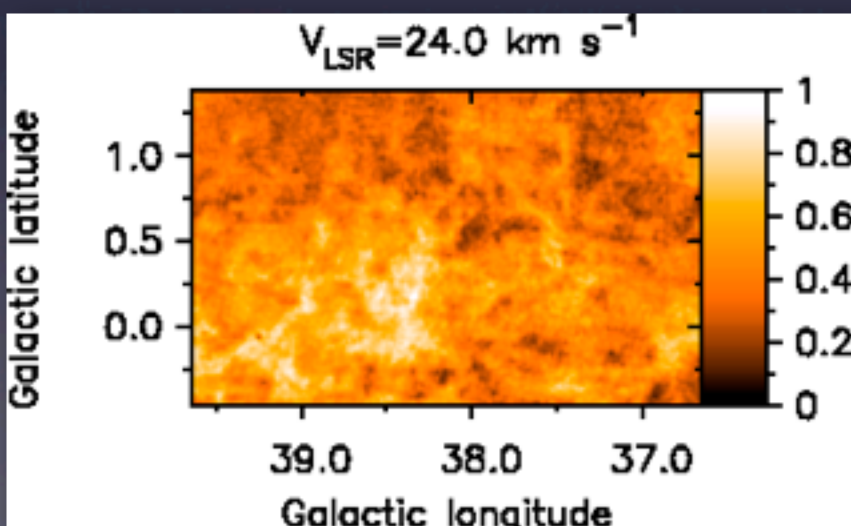

Stil et al, 2006

HI self-absorption in M31
may 'hide' 30% of total HI mass

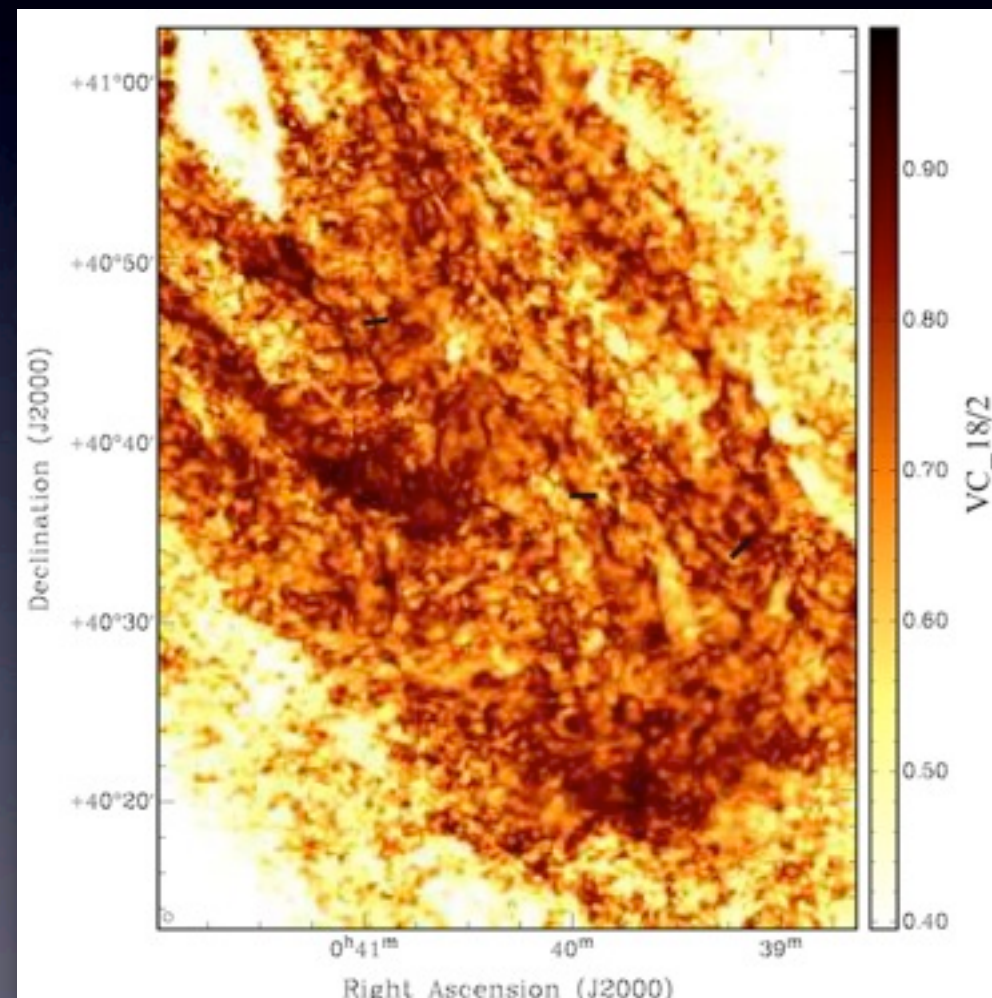

Braun et al 2009

astrophysical MASERs

- Non-thermal, stimulated emission
  - inverting level populationss through pumping
  - extremely high T_b → suitable for VLBI observations
- Occurs under special circumstances in high-density regions:
  - Galactic star formation regions
  - circumstellar envelopes around young and evolved stars
  - starburst galaxies (mega-MASERSs)
- Different MASERs trace different physical conditions
- Most common species:

	GHz	cm
OH	1.612	18.6
	1.665/1.667	18.0
	1.720	17.4

	GHz	cm
H_2CO	4.829	6.21
CH_3OH	12.178	2.46
H_2O	22.235	1.35
SiO	43.122	0.70

astrophysical MASERs

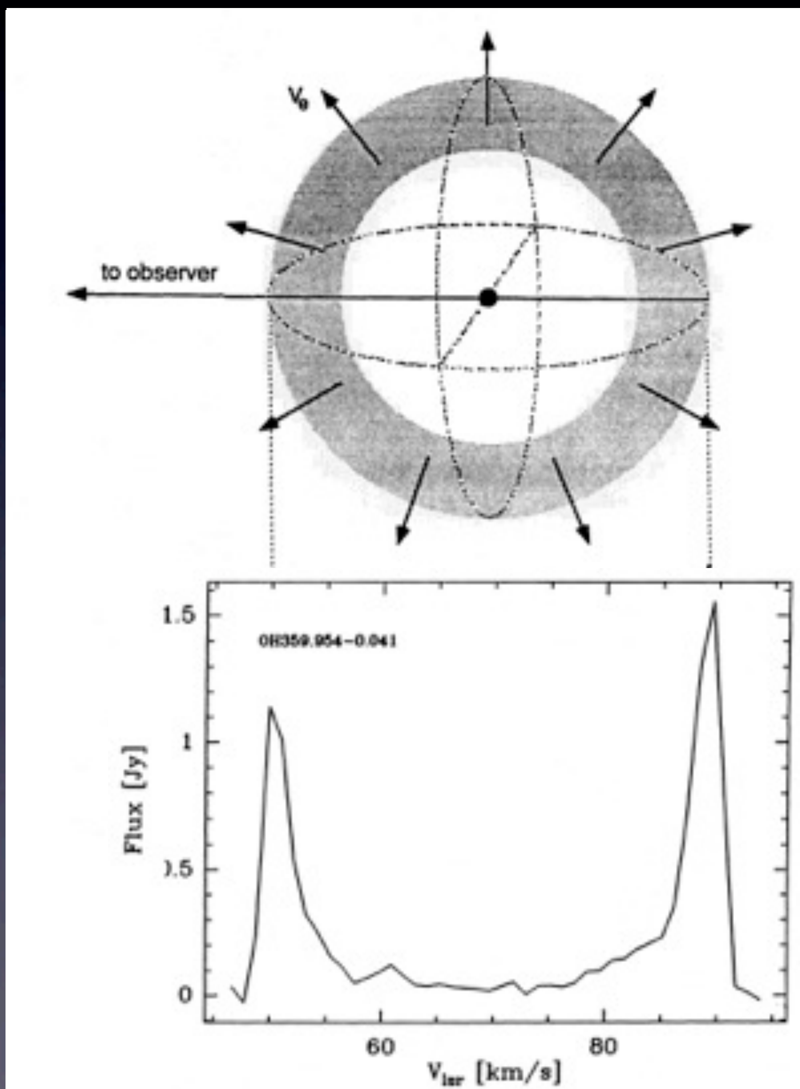

Spaans et al 1992

Double-peaked OH masers first observed in 1968 in AGB stars with mass loss.

Successfully modeled with complex radiative transfer within a thick shell.

Lag in variability between red/blue peak and angular diameter provides distances.

astrophysical MASERs

SiO MASERs around TX Cam
a pulsating AGB star

probe the area between the stellar surface and the dust condensation region.

provides insight in the kinematics of the wind and shocks in relation to stellar pulsations

VLBA, 43GHz, 60 epochs

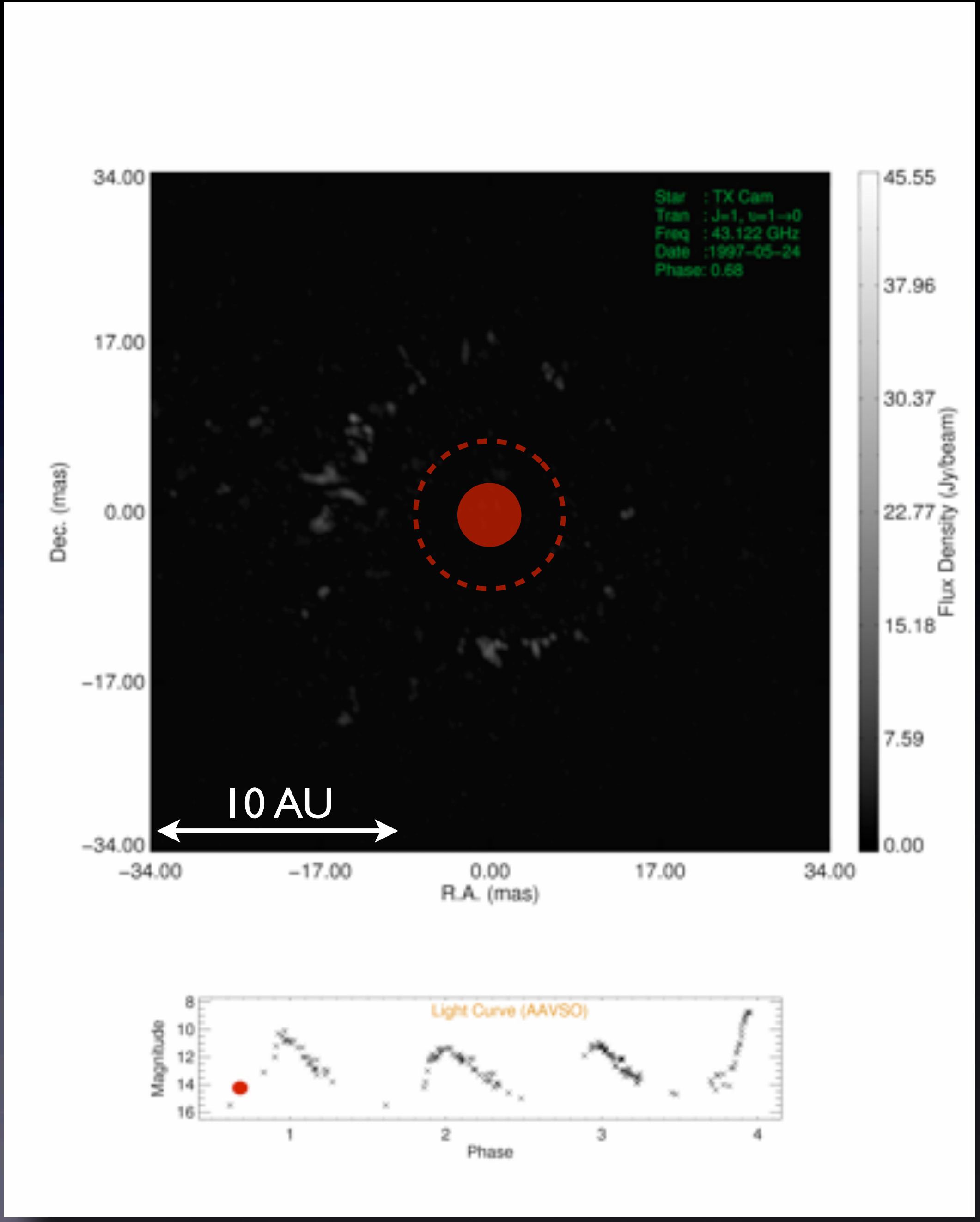

Gonidakis et al 2010

astrophysical MASERs

H_2O masers in a disk around the core of the Seyfert galaxy NGC 4258

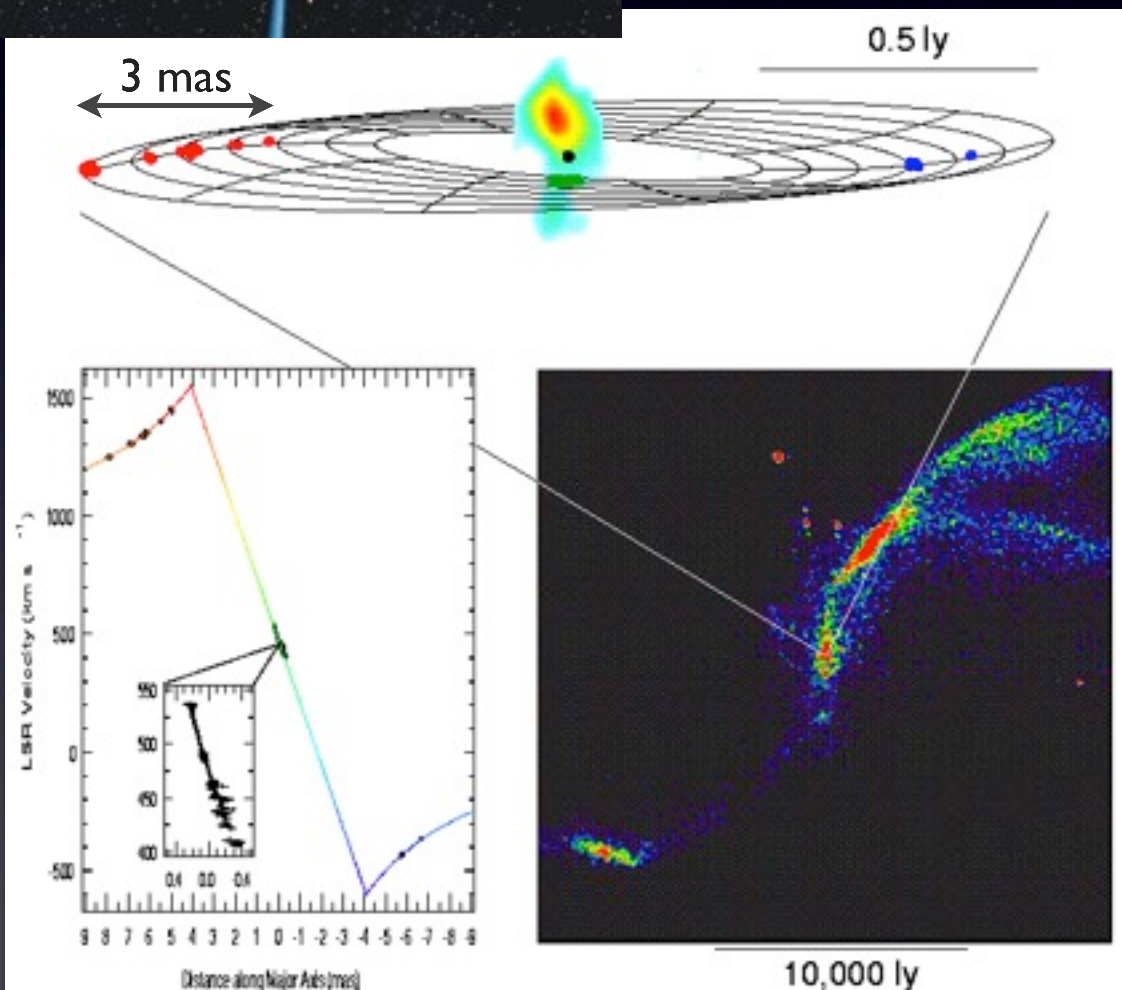

image: J. Moran et al

Keplerian rotation curve, suggests central mass of $4 \times 10^7\ M_\odot$

statistical proper motions of systemic masers provides highly accurate distance of 7.2 ± 0.3 Mpc

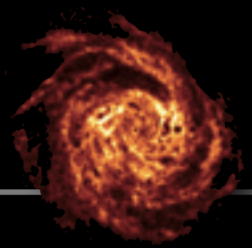

Radio Recombination Lines

- Origin : cascading of electrons after recombination in the diffuse ionized medium.

- Transition in Hydrogen from level (n+Δn)=93 to n=92 is denoted by H92α (α: Δn=1 , β: Δn=2 etc).

  E.g., C576γ denotes a transition in the Carbon atom from energy level n+Δn=579 to n=576.

- RRLs provide information on temperature and electron density, and thus on pressure, of the ISM, as well as degree of ionization, abundances and kinematics.

- Two regimes : RRLs at <1 GHz associated with CNM
  RRLs at >1 GHz originate in HII regions

Radio Recombination Lines

Low frequencies : - Carbon RRLs associated with the diffuse Cold Neutral Medium
- Origin of Hydrogen RRLs less clear

C576α and C576β detected in absorption against the SNR Cas A.

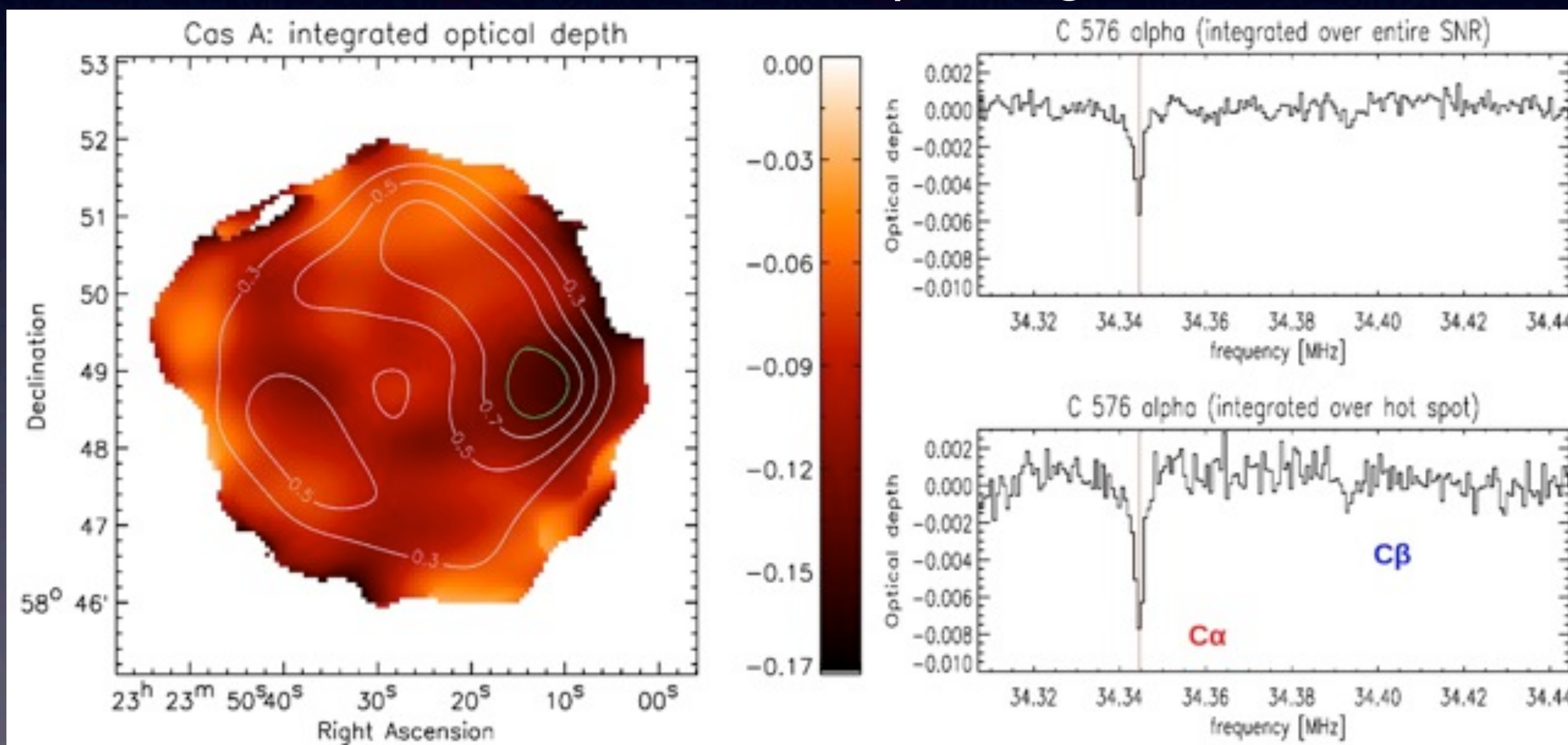

image courtesy by Raymond Oonk

Not yet detected in extragalactic sources

Radio Recombination Lines

High frequencies : - RRLs associated with HII regions
- H, He, C and S are detected
- seen in nearby galaxies like M82, N253,...

broad H92α lines in two HC HII regions

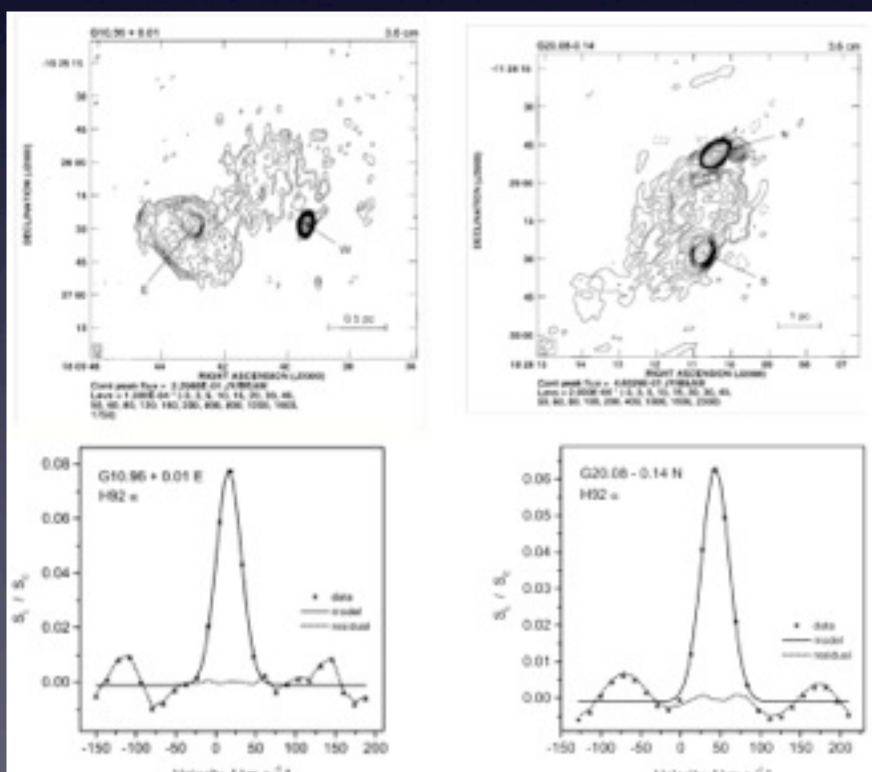

Sewilo et al 2004

H92α in Arp220 with VLA @ 8.1GHz

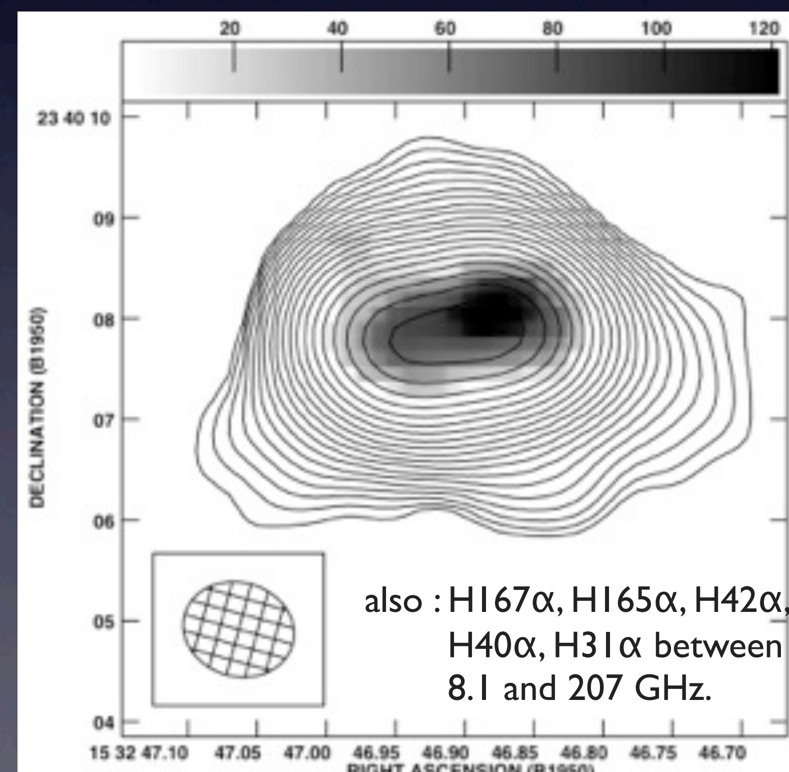

also : H167α, H165α, H42α, H40α, H31α between 8.1 and 207 GHz.

Anantharamaiah et al 2000

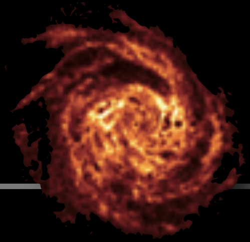

summary

polarimetric

Spectral line ^ aperture synthesis imaging

is the coolest thing in astronomy !